Investigating down-shore migration effects on individual growth and reproduction of the ecosystem engineer Arenicola marina

Lola de Cubber, Sébastien Lefebvre, Théo Lancelot, Gwendoline Duong, Sylvie Marylène Gaudron

Investigating down-shore migration effects on individual growth and reproduction of the ecosystem engineer *Arenicola marina*

Lola De Cubber[a,*], Sébastien Lefebvre[a], Théo Lancelot[a], Gwendoline Duong[a], Sylvie Marylène Gaudron[a,b]

[a] *Univ. Lille, Univ. Littoral Côte d'Opale, CNRS, UMR 8187 Laboratoire d'Océanologie et de Géosciences, F-59000 Lille, France*
[b] *Sorbonne Univ., UFR 918 & UFR 927, 75005 Paris, France*

Abstract

Arenicola marina (Annelida Polychaeta) is a harvested ecosystem engineer inhabiting galleries within soft-sediment foreshores from the Mediterranean to the Arctic. It displays a typical distribution pattern on most foreshores, with the juveniles inhabiting the mediolittoral shore and migrating to the infralittoral shore while growing. In this study, we have characterized the shore migrations of a temperate population of *A. marina* and estimated its potential individual growth and reproduction under different migration scenarios using a Dynamic Energy Budget model. A sand temperature model was developed in order to predict the temperature experienced by lugworms according to the depth of their galleries and their bathymetric level. The food availability and the associated scaled functional response were estimated from *in situ* growth data and associated nitrogen content and chlorophyll-a concentration (Chla) data. The metabolic response of lugworms to temperature (temperature tolerance range, related Arrhenius temperatures) was assessed from literature data. The sand temperature model outputs did not explain alone spatial differences in individual growth and reproduction. However, an increase of food availability with bathymetry, with Chla as a proxy, well explained growth and reproduction. For now, the temperature hypothesis is discarded but other factors (desiccation or hypoxia) should be considered in future studies.

*Corresponding author: lola.decubber@gmail.com

Keywords

Dynamic Energy Budget, Sand temperature model, Lugworm, Metabolic activity and Intertidal ecosystem

1. Introduction

Arenicola marina (L.) is a marine benthic polychaete (Annelida) living in burrows of 5 - 10 cm deep for juveniles and up to 30 cm deep for adults on intertidal coastal sediments, and distributed from the Mediterranean to the Arctic (Longbottom, 1970; Volkenbron, 2005). This polychaete is considered to be an ecosystem engineer, as it creates bioturbation through sediment reworking, enhancing sediment oxygenation by flushing its burrow, selecting species (such as bacteria, microphytobenthos, some amphipods like *Urothoe poseidonis* and copepods) at the expenses of others (such as tube worms or some marine plants like *Zostara noltii*) (Clarke et al., 2017; Kristensen, 2001; Reise, 1985; Volkenborn, 2005). Lugworms are commonly harvested for bait in several countries, where their commercial value can be substantial (De Cubber et al., 2018: Watson et al, 2017), leading to some negative impacts on the associated species or on the harvested *A. marina* population itself (Beukema, 1995; Clarke et al., 2017; Olive, 1993). Consequently, the need for implementing management measures for some populations of *A. marina* has been evidenced in the Eastern English Channel (De Cubber et al., 2018), and some management measures have already been implemented in Europe, such as licensing in the UK (Watson, 2015) or quotas in Portugal (Xenarios et al., 2018).

However, those management measures rarely rely on the local ecology and life-history traits of the species (Watson et al., 2017). *A. marina* displays a benthopelagic life cycle, with larvae dispersing in the water column and temporarily settling for 6 to 7 months on subtidal bottoms (macroalgae and mussel beds), where they live in mucus tubes attached to the substrate and feed on suspended and deposited particles around their tube (De Cubber et al., 2019). Then, a second dispersal phase precedes the lugworms' settlement on the foreshores (considered as the recruitment), where the juveniles and later adults live in galleries and are psammivorous, swallowing the sediment enriched with organic matter (De Cubber at al., 2019; Farke

and Berghuis, 1979a, b; Newell, 1948; 1949; Reise, 1985; Reise et al., 2001). Recently, a Dynamic Energy Budget (DEB) model has been developed by De Cubber et al. (2019) in order to explore the time scale of the appearance of the different life-stages of *A. marina*. DEB models enable to predict individual growth and reproduction of a species as well as several of its life-history traits (age at metamorphosis, puberty, etc.) according to the environmental conditions (temperature and food) by quantifying the energy fluxes (Kooijman, 2010). Therefore, when local environmental conditions (temperature and food resources) are known, the DEB models can provide valuable data on the biology of a targeted species to help managers to implement management measures.

Up to now, the DEB model implemented for *A. marina* only considered changing environmental conditions for the early life-stage phases (before recruitment) (De Cubber et al., 2019). For juveniles and adults, mean (constant) environmental conditions (seawater temperature and food proxy) have been used as forcing variables to run the DEB model (De Cubber et al., 2019). However, since lugworms live within the intertidal area, they experience daily temperature variations (De Cubber et al., 2019) that may be highly variable according to their location on the shore (bathymetric level) and to the depth of their gallery. Specific physiological and behavioural responses of intertidal species may be triggered by heat stress such as seen in the mussel *Mytilus californianus*, where outside its optimal temperature tolerance range, a decrease of its physiological performances has been revealed (Kish et al., 2016) or in the gastropod *Echinolittorina malaccana*, where outside its optimal temperature tolerance range, tower formation has been observed (Seuront and Ng, 2016). Theses responses appear crucial to be taken into account when considering the metabolism of intertidal species. As a matter of fact, the distribution of juvenile and adult lugworms on the foreshore is not random and has been widely documented, describing juveniles recruiting on the high mediolittoral part of the shore and gradually migrating down to the high infralittoral part of the shore (Cadman, 1997; De Cubber et al., 2019, 2018; Farke et al., 1979; Reise, 1985; Reise et al., 2001). Some exceptions of this distribution in some sites may occur, where individuals are almost only present on the lower mediolittoral to high infralittoral foreshore (De Cubber et al., 2018).

Understanding the dynamic of the distribution of the lugworm population might be vital for further population dynamic models studies (Martin et al., 2012), used by managers to conduct their management plans.

Several hypotheses have been raised to explain the down-shore migration of lugworms. First, environmental conditions (temperature and food resources) may be more favourable to lugworms in the infralittoral compared to the high mediolittoral (Flach and Beukema, 1994). Second, lugworms may migrate down the shore to escape intra-specific competition for space and food (Farke et al., 1979; Flach and Beukema, 1994; Longbottom, 1970; Reise at al., 2001). Finally, inter-specific competition and predation might also happen (Farke et al., 1979). On the foreshore, the temperature experienced by organisms is driven by the seawater temperature during immersion and by the air temperature, solar radiation, wind, air humidity and atmospheric pressure during emersion (Guarini et al., 1997). Models aiming at simulating the temperature of sediment have already been implemented by several authors in the case of mudflats (Guarini et al., 1997; Savelli et al., 2018). They rely on the heat energy balance of the different fluxes applied to the sediment surface, and on the parameters of the sediment (Guarini et al., 1997; Savelli et al., 2018). Nevertheless, this has never been done yet for a sandy habitat on the foreshore to our knowledge. In the present study, we tested the hypothesis that temperature and food levels were the main forcing variables driving the lugworms to migrate down the shore using a DEB model. Our specific objectives were:

1. to characterize the *in situ* shore migrations of a local population of *A. marina*,
2. to reconstruct the sand temperature of the shore according to the depth of the galleries and the bathymetric level, as well as to measure local food levels,
3. to estimate the metabolic response of lugworms to temperature (via the Arrhenius temperature) and to different proxies for food sources and quantities (via the scaled functional response) using a DEB model,
4. to compare the potential for growth and reproduction of *A. marina* individuals under different migration scenarios using a DEB model.

2. Material and Methods

2.1. Study area

Lugworms and the associated environmental parameters were collected at Wimereux (N 50°46'14", E 01°36'38"), located on the Eastern English Channel (Hauts-de-France, France) (Fig. 1). The area is composed of a mixture of sandy and rocky bottoms, and the tidal regime is semi-diurnal and macrotidal with amplitudes that may exceed 8 m around 2 days before the full moon (Migné et al., 2004; Rolet et al., 2015). In this area, the population of *Arenicola marina* is mainly found on the high mediolittoral to low mediolittoral/infralittoral part of the foreshore and therefore exposed to emersion periods of several hours (De Cubber et al., 2018).

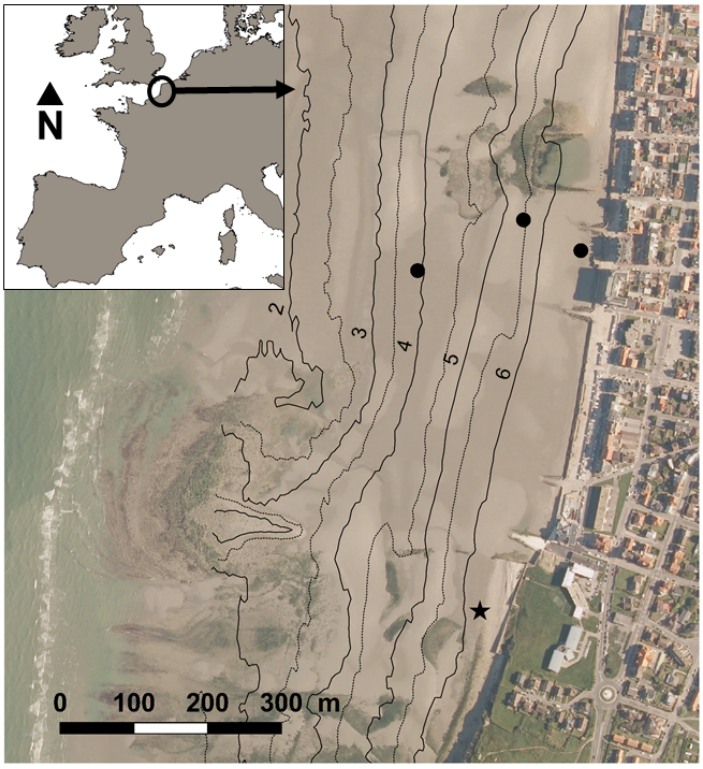

Figure 1: Study site of Wimereux (Eastern English Channel, France) and location of the sampling points for the sediment temperature measurements with two HOBO® Water Temp Pro v2 probes fixed on a metal rod embedded in the sediment (star), and for the size structure of the *Arenicola marina* population (dots) on different bathymetric levels (lines with numbers) of the foreshore.

Densities of *A. marina* have been reported to range from 0 to 61 individuals.m^{-2} with the greatest density on the high mediolittoral shore constituted by smaller

individuals. More details on the study site and the population of *A. marina* of the area are given in De Cubber et al. (2018).

2.2. Compilation of in situ observations

A dataset of physical measurements collected within the area of the study site was compiled to force a sediment temperature model based on the one developed by Guarini et al. (1997) for mudflats (Fig. 2). The wind speed U ($m.s^{-1}$), the air temperature T_{Air} (K), the relative humidity H_r (%), the atmospheric pressure P_{atm} (Pa) and the irradiance R_s ($J.m^{-2}$) were extracted from environmental data recorded hourly at Boulogne-sur-Mer (N 50°43'35", E 01°36'53") (wind speed, air temperature, relative humidity and atmospheric pressure) and Calais (N 50°56'53", E 01°51'23") (irradiance) (France) by Meteo France ltd. (https://donneespubliques.meteofrance.fr/) during the years 2017 and 2018. The water height H_w (m) (Fig. 2) was obtained for the same years from the Marel Carnot station (http://www.ifremer.fr/coen/eulerianPlatform) at the tide gauge of Boulogne-sur-Mer. The water height was compared to the elevation of the three shore points (Fig. 1), obtained from the interregional project CLAREC, INSU-CNRS M2C-UNICAEN (http://www.uni caen.fr/dataclarec/home/elevations.html) according to the local marine altimetric references (SHOM, 2017).The water temperature T_w (K) consisted in hourly measurements from the same Marel Carnot station coupled with monthly observations made by the Service d'obs-ervation en milieu littoral (SOMLIT, http://somlit-db.epoc.u-bordeaux1.fr/bdd.php) at Wimereux (coastal bottom point), when data of the Marel Carnot station were missing. The chlorophyll-a concentration of the seawater *Chla* ($\mu g.L^{-1}$) was also retrieved from the Service d'observation en milieu littoral (SOMLIT) at Wimereux (coastal point) in order to be tested as a proxy of the food levels.

2.3. Field sampling and laboratory measurements

Follow-up of the Arenicola marina population structure at Wimereux. From March 2017 to July 2018, around 30 individuals of *A. marina* were sampled 8 times at each of the three locations on the foreshore from the mediolittoral/infralittoral to high mediolittoral at the study site (Fig. 1).

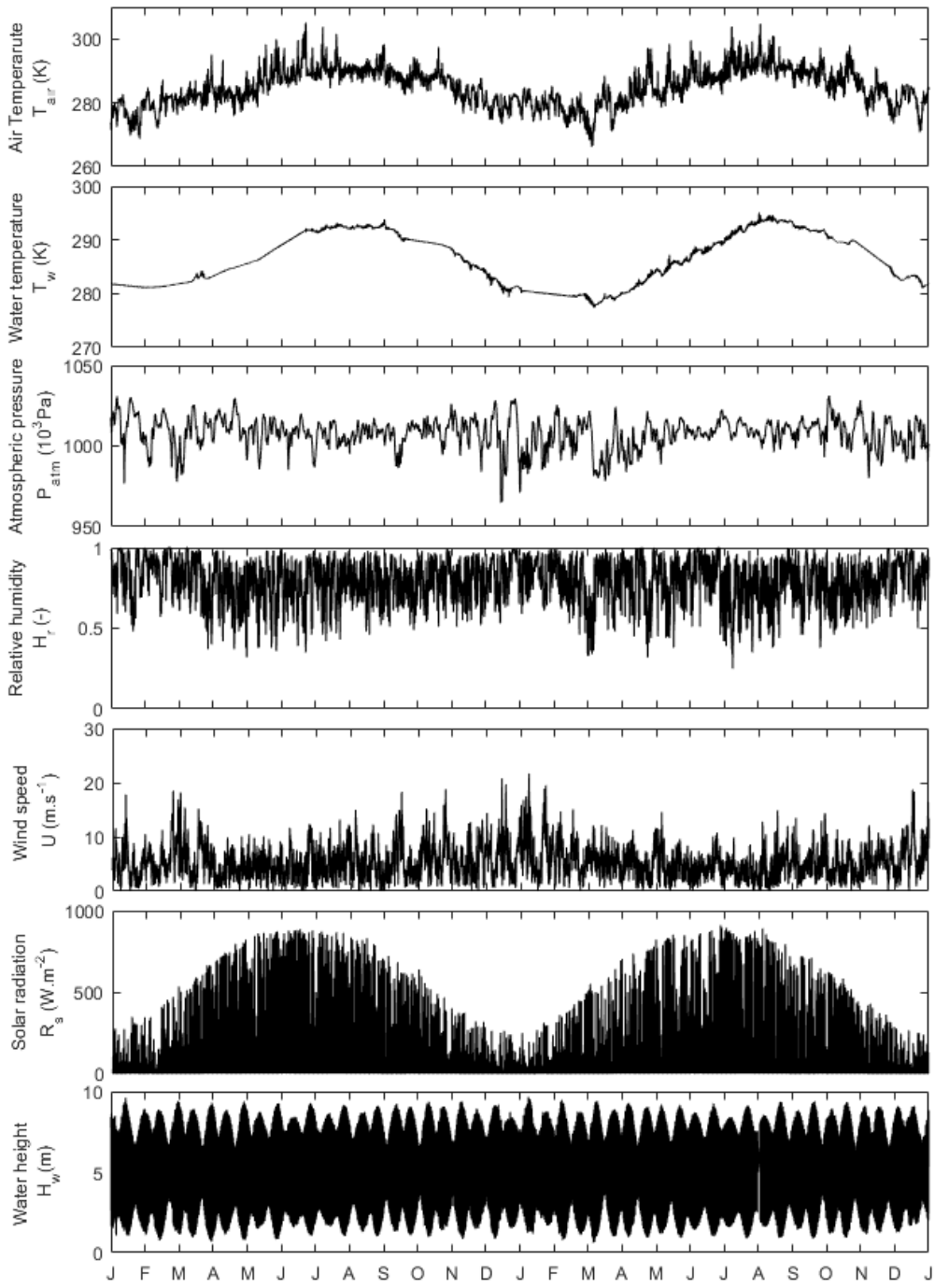

Figure 2: *In situ* air temperature (T_{air}, K), seawater temperature (T_w, K), atmospheric pressure (P_{atm}, 10^3.Pa), relative humidity (H_r, -), windspeed (U, m.s^{-1}), solar radiation (R_s, W.m^2) and water height (H_w, m) used as forcing variables to constrain the sediment temperature model between January 2017 and December 2018. The data were recovered from the Marel Carnot station (H_w, T_w) (http://www.ifremer.fr/co-en/eulerianPlatform), Meteo France ltd. (T_{air}, P_{atm}, H_r, U, R_s) (https://donneespubliques.meteofrance.fr/), and the Service d'observation en milieu littoral (SOMLIT, http://somlit-db.epoc.u-bord eaux1.fr/bdd.php) at Wimereux (coastal bottom point) (T_w). The seawater temperature T_w was reconstructed from both the Marel Carnot station when data were available (high-frequency measurements) and SOMLIT otherwise (low frequency measurements).

There, the population of *A. marina* has already been shown to display the typical spatial distribution (De Cubber et al., 2018) described by other authors with juveniles on the higher shore and adults elsewhere (Farke et al., 1979).

Follow-up of the nitrogen content of sediment. Triplicates of surface sediment cores (1 cm deep x 10 cm of diameter) were collected at the same three locations of the study site at every sampling period (n = 8) in order to assess the organic matter content of the sediment. Once collected, samples were kept at -20°C until analysis. Homogenised aliquots of around 30 g of each of the subsamples were then put in separate tin containers and analyzed with an organic elemental analyzer Thermofisher Flash 2000 after calibration, in order to measure the nitrogen content of sediment. For each sample, one subsample was burnt during 5 h at 550°C in order to remove the organic nitrogen, and another one was dried out at 40°C during 1 day. The calibration was performed by analyzing the nitrogen content of several sediment samples for which the elemental contents were known. Given the low nitrogen concentrations of the sediment and the detection levels of the device, only the total nitrogen content (organic + inorganic) of the sediment could be measured.

Follow-up of the temperature variations within the sediment. Temperatures within the sediment (*ca* 5 cm and 21 cm deep) were recorded with two HOBO® Water Temp Pro v2 probes fixed on a metal rod embedded in the sediment on the higher shore (high mediolittoral) of the study site between the 01/10/17 and the 24/10/17 and between the 03/05/18 and the 01/07/18 (10 min interval between each measurement) (Fig. 1).

2.4. Data analysis

2.4.1. Sediment temperature model

The model. The sediment temperature model helped to solve the sediment temperature (T_s) equation adapted from Guarini et al. (1997), where t is the time (s), z is the depth (m), η is the heat conductivity (W. m^{-1}. K^{-1}) and μ is the thermal diffusivity (m^2. s^{-1}) of the sediment (Equation 1).

$$\frac{\eta}{\mu} \cdot \frac{\delta T_s(z,t)}{\delta t} = \frac{\delta}{\delta z} \cdot \eta \cdot \frac{\delta T_s(z,t)}{\delta z} \quad (1)$$

The partial differential equation was solved on Matlab 2015b using the pdepe function considering heat energy balance equations at the boundaries $z_0 = 0$ m (sediment surface) and $z_1 = 1$ m deep (beyond this depth, the sediment temperature is supposed equal to the one of the water) (Tables 1, 2).

Table 1: Equations of the heat energy balance at the boundary conditions (Guarini et al, 1997) and the associated heat fluxes (Brock et al., 1981; Guarini et al., 1997; Savelli et al., 2018) as implemented in the present study.

Heat Energy balance equations at the boundary conditions		
	immersion	emersion
$z_0 = 0$ m	$f_{HEB}\left(T_s(0,t)\right) = S_{s-w}$	$f_{HEB}\left(T_s(0,t)\right) = R_{sun} + R_{atm} - R_s - S_{s-a} - V_s$
$z_1 = 1$ m	$f_{HEB}\left(T_s(1,t)\right) = -S_{s-w}$	$f_{HEB}\left(T_s(1,t)\right) = -S_{s-w}$
Heat fluxes (W.m^{-2}) equations		
Solar radiation	$R_{sun} = R_{obs}$	
Atmosphere radiation	$R_{atm} = \epsilon_a \cdot \sigma \cdot T_{air}^4 \cdot (\zeta - k)$	
	$\epsilon_a = 0.937 \cdot 10^{-5} \cdot T_{air}^2$	
	$k = R_{obs}/R_{std}$	
	$decl = 23.45 \cdot sin\left(360 \cdot \frac{284 + day_{julian}}{365}\right)$	
	$R_1 = \left(\sqrt{1 + 0.33 \cdot cos\left(\frac{360 \cdot day_{julian}}{365}\right)}\right)^{-1}$	
	$cos_z = sin(decl) \cdot sin(latitude) + cos(decl) \cdot cos(latitude) \cdot cos((hour_{light} - 12) \cdot 15)$	
	$R_{std} = R_0 \cdot \frac{cos_z}{2 \cdot R_1^2} \cdot \left(1 + cos(\frac{2 \cdot \pi \cdot (hour - 1)}{length_{daylight}}\right)$	
Sand radiation	$R_s = \epsilon_M \cdot \sigma \cdot T_s(z_0,t)^4$	
Sand-air heat conduction	$S_{s-a} = \rho_a \cdot C_{Pa} \cdot C_b \cdot (1+U) \cdot (T_s(z_0,t) - T_{air})$	
Evaporation	$V_s = \xi \cdot \rho_a \cdot L_V \cdot C_V \cdot (1+U) \cdot (q_s \cdot (1 - q_a/q_s))$	
	$L_V = (250.84 - 2.35 \cdot (T_s(z,t) - 273.15)) \cdot 10^3$	
	$q_s = \frac{\lambda \cdot p_{sat}^V}{p_{atm} - (1-\lambda) \cdot p_{sat}^V}$	
	$p_{sat}^V = exp\left(2.3 \cdot \left(\frac{7.5 \cdot (T_{air} - 273.15)}{237.3 + (T_{air} - 273.15)} + 0.76\right)\right)$	
Sand-water heat conduction	$S_{s-w} = -\frac{\eta}{h_w} \cdot (T_s(z_0,t) - T_w(t))$	

At emersion time, the surface temperature was calculated from the heat energy balance between the solar radiation, the atmosphere radiation, the sand radiation, the sand-air heat conduction and the evaporation fluxes, and the 1 m depth temperature from the sand-water heat conduction flux (Tables 1, 2) (Guarini et al., 1997; Savelli et al., 2018). At immersion time, both the surface and the 1 m depth

temperatures were calculated from the sand-water heat conduction flux (Tables 1, 2) (Guarini et al., 1997).

Table 2: Parameters values and their references used in the sediment temperature model as implemented in the present study.

Parameters of the model		References
Thermal diffusivity of the sand*	$\mu = 5.2164 \cdot 10^{-7}$ m^2.s^{-1}	Calibrated in this study
Conductivity of the sand*	$\eta = 3.3182$ W.m^{-1}.K^{-1}	Calibrated in this study
Constant*	$\zeta = 1.2118$ -	Calibrated in this study
Stephan-Boltzman constant	$\sigma = 5.67 \cdot 10^{-8}$ -	Guarini et al. (1997)
Sand emissivity	$\epsilon_M = 0.96$ -	van Bavel and Hillel (1976)
Bulk coefficient for conduction	$C_b = 0.0014$ -	Guarini et al. (1997)
Sand porosity	$\xi = 0.351$ -	Rauch and Denis (2008)
Solar constant	$R_0 = 1353$ W.m^{-2}	Brock et al. (1981)
Bulk coefficient for evaporation	$C_V = 0.0014$ -	Guarini et al. (1997)
Air volumetric mass	$\rho_a = 1.2929$ kg.m^{-3}	Guarini et al. (1997)
Specific air heat	$C_{Pa} = 1003$ J.kg^{-1}.K^{-1}	Guarini et al. (1997)
Constant evaporation ratio	$\lambda = 0.621$ -	Guarini et al. (1997)

* Parameters estimated in this study to fit the model predictions to observations

Validation of the model. The parameters related to the sediment type for which no data for sandy sediments were available (η, μ, and ζ) were estimated comparing the model output with our *in situ* sediment temperature measurements (HOBO® probes) for two recording periods (Table 2). The estimation procedure was performed on Matlab 2015b using the fminsearch function. For each period, three tidal cycles of one emersion and one immersion period (approximately 36 hours) were chosen randomly among all, 23 times for the first and shortest *in situ* temperature recording period (October 2017, 36 cycles in total) and 63 times for the second *in situ* temperature recording period (May-June 2018, 107 cycles in total). The estimation procedure was applied to these periods minimizing the mean square error (MSE) between the data and the model predictions. For each *in situ* temperature recording period, the mean parameter value was computed as well as its standard deviation. These two means were compared with a non-parametric Krukal-Wallis test performed on Matlab R2015b. The mean value of these means was used as parameter value in the implementation of the model. The parameter values obtained were then used to compute the sediment temperature on the three sampled shore levels from the surface to 1 m deep as well as the daily mean and variance of the sediment temperature at these depths.

2.4.2. Effect of temperature on the metabolic rates of Arenicola marina

All metabolic rates depend on temperature (Kooijman, 2010). Within the species-specific temperature tolerance range, the effect of temperature on metabolic rates can be described with the Equation (2), with T the temperature (K), T_{ref} the reference temperature (taken to be 293.15 K), T_A the Arrhenius temperature (K), $\dot{k}_1$ the rate of interest at T_{ref}, and $\dot{k}$ the computed rate at T. Outside the lower and higher boundaries of the species-specific temperature tolerance range (respectively T_L and T_H), the effect of temperature on metabolic rates changes and is calculated adding an extra term to the Equation (2) as presented in Equation (3), with T_{AL} the Arrhenius temperature below the lower boundary of the species-specific temperature tolerance range (K) and T_{AH} the Arrhenius temperature above the higher boundary of the species-specific temperature tolerance range (K) (Kooijman, 2010).

$$\dot{k}(T) = \dot{k}_1 \cdot \exp\left(\frac{T_A}{T_{ref}} - \frac{T_A}{T}\right) \tag{2}$$

$$\dot{k}(T) = \dot{k}_1 \cdot \exp\left(\frac{T_A}{T_{ref}} - \frac{T_A}{T}\right) \cdot \frac{1 + \exp\left(\frac{T_{AL}}{T_{ref}} - \frac{T_{AL}}{T_L}\right) + \exp\left(\frac{T_{AH}}{T_H} - \frac{T_{AH}}{T_{ref}}\right)}{1 + \exp\left(\frac{T_{AL}}{T} - \frac{T_{AL}}{T_L}\right) + \exp\left(\frac{T_{AH}}{T_H} - \frac{T_{AH}}{T}\right)} \tag{3}$$

The Arrhenius temperature of *A. marina* has been previously estimated, using equation 2, together with the other DEB parameters with the DEBTool package (De Cubber et al., 2019; Marques et al., 2018). However, the temperature tolerance range of the species, as well as the Arrhenius temperatures outside its temperature tolerance range, has not been estimated yet given that no data below 5 °C and above 20 °C were used in the previous DEB parameter estimation (De Cubber et al., 2019). Hence, new data outside this temperature range were added to the former dataset to allow to re-estimate the Arrhenius temperature of *A. marina* within its temperature tolerance range T_A and to estimate the boundaries of the temperature tolerance range, T_L and T_H, and the related Arrhenius temperatures, T_{AL} and T_{AH}, as well as the whole parameters set for the species. The new data set consisted in one growth experiment (De Wilde and Berghuis, 1979), one fertilization success experiment (Lewis et al., 2002), one oxygen consumption experiment (Schröer et al., 2009) and one mitochondrial respiration experiment (Sommer and Pörtner, 2004),

all four at several temperatures. The whole DEB parameters (including T_A, T_L, T_H, T_{AL} and T_{AH}) were re-estimated using the DEBTool software on Matlab R2015b (Marques et al., 2018).

2.4.3. Estimation of in situ growth and scaled functional response reconstruction

For each sampling date, the population structure was approached through the analysis of size frequencies on the trunk length (TL) with a 5-mm size class interval, using a Bhattacharya analysis (De Cubber et al., 2018). Each cohort belongs to a separate year since spawning and recruitment only happen once a year (De Cubber et al., 2018). In order to reconstruct the actual temperature experienced by the collected lugworm, the mean depth of the lugworms between each sampling date was assessed using the linear relation presented in Equation (4), with TL (cm) the mean trunk length of the cohort and z (cm) the associated depth of the gallery (considering that juveniles of 1 cm of trunk length dig a gallery of 5 cm of depth while adults of 12 cm of trunk length dig a gallery of 30 cm of depth). The mean sediment temperature at this depth was then calculated with the sand temperature model assuming a bathymetric level obtained from Equation 6 (Fig. 10).

$$z = 30 - 25 \cdot \frac{12 - TL}{12 - 1} \tag{4}$$

The new DEB parameters for *A. marina* were used to model the growth and reproduction of the lugworms according to the *in situ* sediment temperature previously estimated. The growth before recruitment (or up to metamorphosis) was reconstructed using the environmental conditions detailed in De Cubber et al. (2019) to recreate relevant initial conditions of the growth of recruits once settled. From metamorphosis time, between each collection date, the trunk length growth was reconstructed using the DEB equations detailed in De Cubber et al. (2019) for a scaled functional response f varying from 0.01 to 1. The scaled functional response enabling the best fit (with the lowest mean squared error MSE between growth observations and predictions) was then used as the mean scaled functional response for this time step.

2.4.4. Linking the scaled functional response to food resources

The mean total nitrogen content of sediment available for the recruits was reconstructed from values of the total nitrogen content obtained from each bathymetric level of the shore and the relative contribution of each bathymetric level to the total recruits cohorts. The mean concentration of chlorophyll-a and the reconstructed total nitrogen content of sediment each interval between sampling events corresponding to one reconstructed f level were tested as proxy of food density. The relation between the scaled functional response and the food density X (chlorophyll-a concentration or nitrogen content) is presented in Equation (5), where X_K is the half-saturation coefficient (Kooijman, 2010). For the mean chlorophyll-a concentration, the value of X_K was fitted using Equation (5) as the value for which the lowest MSE value between simulations and observations was obtained.

$$f = \frac{X}{X + X_K} \tag{5}$$

2.4.5. Effects of variations in environmental conditions on the small-scale migration patterns of Arenicola marina after recruitment

Several scenarios (n = 18 in total) were tested in order to assess the impact of food and temperature conditions (according to the lugworm shore location and the depth of its gallery) on the individual growth and reproduction of *A. marina* (Fig. 3). Environmental conditions over 1.5 years were reconstructed from the 2-years reconstructed sediment temperature, the 2-year Chla measurements and the half-saturation coefficient (X_K) previously estimated. The associated temperature corrections and functional response were applied to the abj-DEB model for *A. marina* developed by De Cubber et al. (2019), allowing predictions on the trunk length, wet weight and egg number. The spawning event was triggered when the total wet weight of the eggs reached 10 % of the total wet weight according to predictions on growth under constant environmental conditions with annual spawning events made by De Cubber et al. (2019). The initial conditions at metamorphosis (after which juveniles recruit) were estimated at environmental conditions given by De Cubber et al (2019). Three main scenarios were envisioned:

(1) lugworms were supposed to recruit on the high mediolitoral shore without

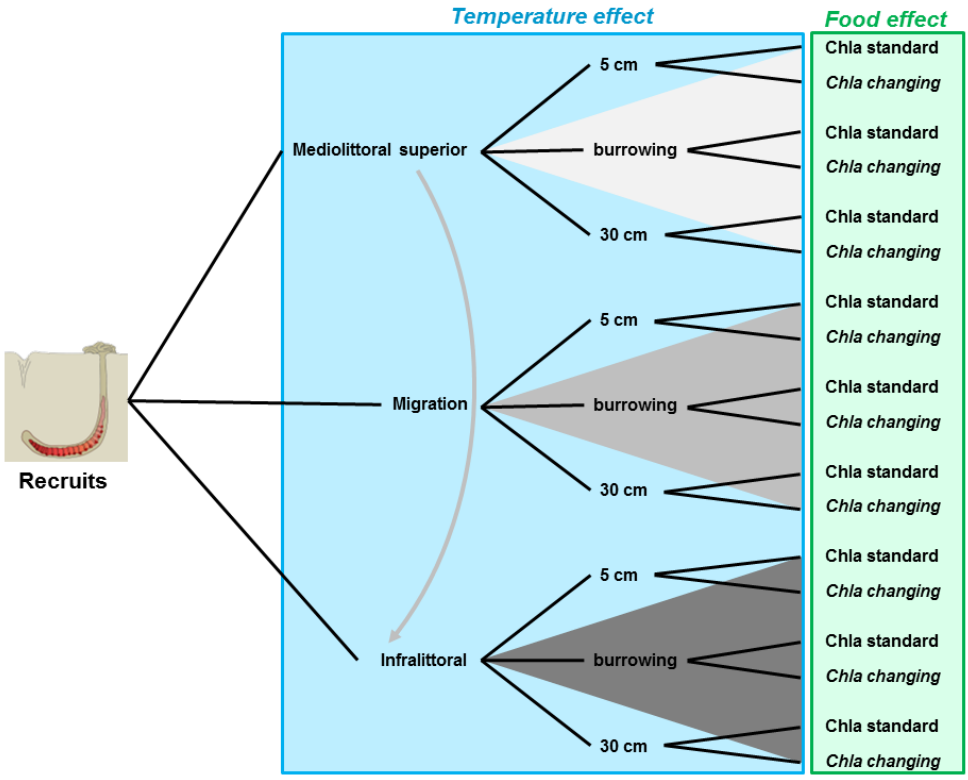

Figure 3: Representation of the different scenarios. In the light grey scenarios, lugworms recruit on the high mediolittoral shore without migrating. In the medium grey scenarios, lugworms migrate according to the Equation (4). In the dark grey scenarios, lugworms recruit directly on the infralittoral shore. For these three options, lugworms remain burrowed at 5 or 30 cm, or are able to burrow from 5 to 30 cm according to the Equation (4). For all these scenarios, we considered on the one hand that chlorophyll-a concentrations were the same everywhere on the shore, or on the other hand that chlorophyll-a concentrations were divided by 2 on the higher shore compared to the lower shore, increasing linearly between these two locations.

299 migrating

300 (2) lugworms were supposed to migrate according to the Equation (4) and the
301 bathymetry-size relation shown in Fig. 10 (Equation 6)

302 (3) lugworms were supposed to recruit directly on the infralittoral shore (Fig. 3)

303 For these three options, lugworms remained burrowed at 5 or 30 cm, or were
304 able to burrow from 5 to 30 cm according to the Equation (4). Finally, for all
305 these scenarios, we considered on the one hand that chlorophyll-a concentrations
306 were the same everywhere on the shore, or on the other hand that chlorophyll-a
307 concentrations were divided by 2 on the higher shore compared to the lower shore,
308 increasing linearly between these two locations. The effects of the change of food

and temperature were estimated by comparing the different DEB model outputs ran with those scenarios (Fig. 3).

3. Results

3.1. Spatial distribution of trunk length frequencies

The spatial distribution of trunk length frequencies present the common pattern usually observed on the shore with smaller individuals close to the coast line and larger ones down the shore (Fig. 4).

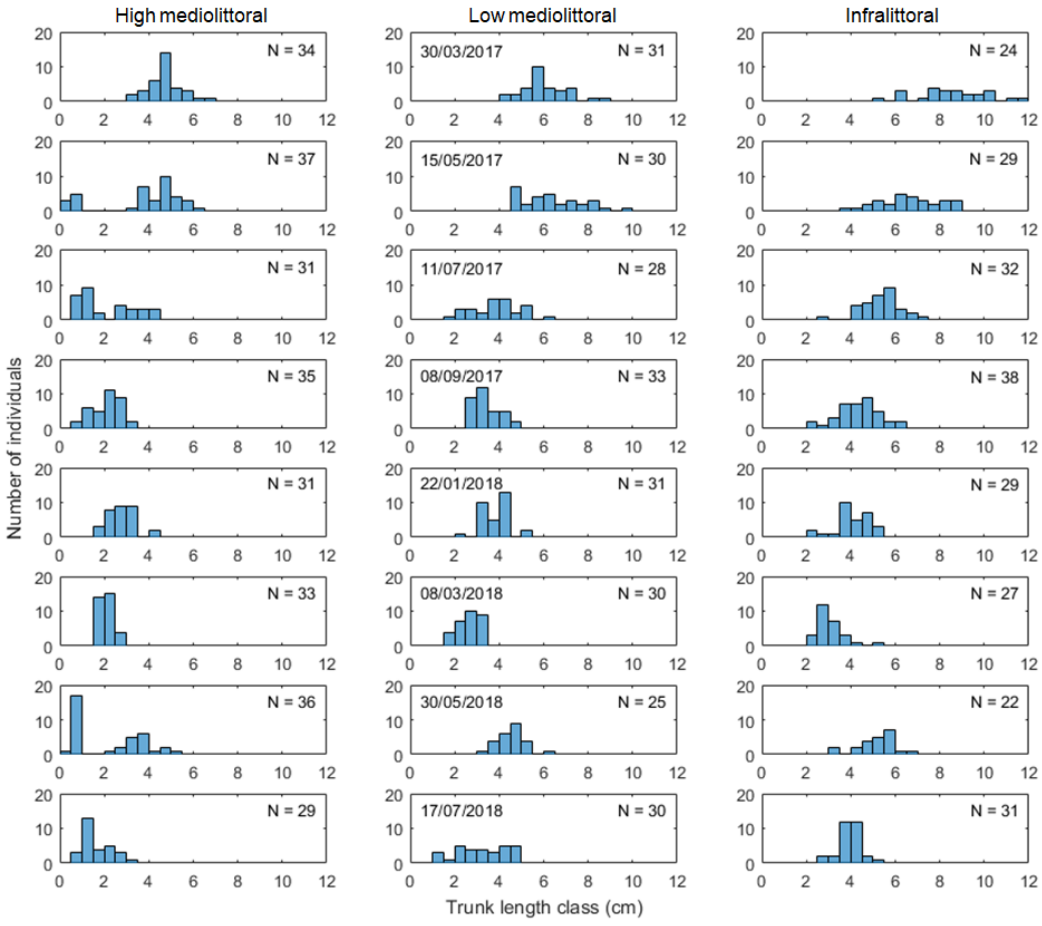

Figure 4: Distribution of the trunk length frequencies of *Arenicola marina* on the high mediolittoral (left), low mediolittoral (middle) and infralittoral (right) at the study site (Wimereux, Eastern English Channel) for each sampling date from the 30/03/2017 to the 17/07/2018. N stands for the number of individuals collected.

For both years, recruitment happened after March and before the end of May. The largest trunk classes (from 8 to 10 cm of trunk length) were mainly represented at the infralittoral sampling point but disappeared after mid May 2017. On the

high mediolittoral shore, some larger trunk length classes disappeared from one sampling event to the next (Fig. 4, for example between May 2018 and July 2018, the individuals larger than 3.5 cm disappeared from the high mediolittoral but were still found lower on the shore). This might be due to mortality, or more probably, small scale migrations down the shore.

3.2. Temperature within the sediment

Validation of the sediment temperature model. The mean fitted values of the constant ζ, the thermal diffusivity μ, and the conductivity η were respectively 1.21, 5.22 e^{-07} m^2.s^{-1} and 3.32 W.m^{-1}.K^{-1} (Table 3). The mean values of ζ and η did not show any significant differences if both parameters were estimated to fit the observations from October 2017 or the ones from May-June 2018 (Kruskal-Wallis test, $p > 0.05$). However, there was a significant difference between the value of μ estimated to fit the observations from October 2017 (5.33 e^{-07} m^2.s^{-1}) and the one estimated to fit the observations from May-June 2018 (5.10 e^{-07} m^2.s^{-1}) (Kruskal-Wallis test, $p < 0.05$) (Table 3, Fig. 5).

Table 3: Mean values of the fitted parameters ζ (constant, no unit), μ (thermal diffusivity, m^2.s^{-1}), and η (conductivity, W.m^{-1}.K^{-1}) and associated standard errors for each of the *in situ* measurement periods (October 2017 and May-June 2018) and both periods using their means. The p-values of the Kruskal-Wallis tests between the values of the two periods are also given.

Mean estimated value	October 2017	May-June 2018	p-value	**All periods**
η (W.m^{-1}.K^{-1})	3.29 ± 0.22	3.35 ± 0.33	0.24	$\mathbf{3.32 \pm 0.29}$
μ (m^2.s^{-1})	$5.33e^{-07} \pm 4.79e^{-08}$	$5.10e^{-07} \pm 4.72e^{-08}$	0.04	$\mathbf{5.22e^{-07} \pm 5.02e^{-08}}$
ζ (-)	1.19 ± 0.19	1.23 ± 0.14	0.63	$\mathbf{1.21 \pm 0.17}$

The estimated mean parameter values of η, μ and ζ provided a good fit of the sediment temperature model for the May-June 2018 sediment temperature observations at 5 cm deep and at 20 cm deep (Fig. 6 c, d). The fit was somewhat less good when considering the sediment temperature observations of October 2017 at both depths but still captured the main trends of temperature variations (Figs. 6 a, b).

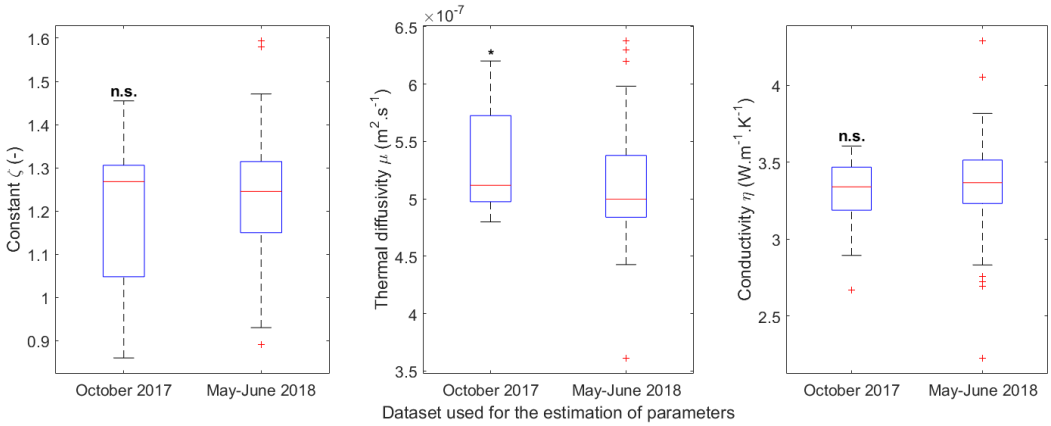

Figure 5: Boxplot representations of the distribution of the fitted values of the constant ζ (-, left), the thermal diffusivity μ ($m^2.s^{-1}$, middle), and the conductivity η ($W.m^{-1}.K^{-1}$, right). For each parameter, the red line is the median of the 23 values obtained for October 2017 and 63 values obtained for May-June 2018 when fitting the model predictions to the observations on a random period of approximately 36 hours. 50% of the values are comprised in the box, 95% in the range between the error bars. The red crosses are extreme values and the black star stands for the significant difference between the values of μ of each of the two recording periods. 'n.s' is indicated when no significant difference was found between the value of a given parameter between the two temperature recording period.* indicates a significant difference ($p < 0.05$).

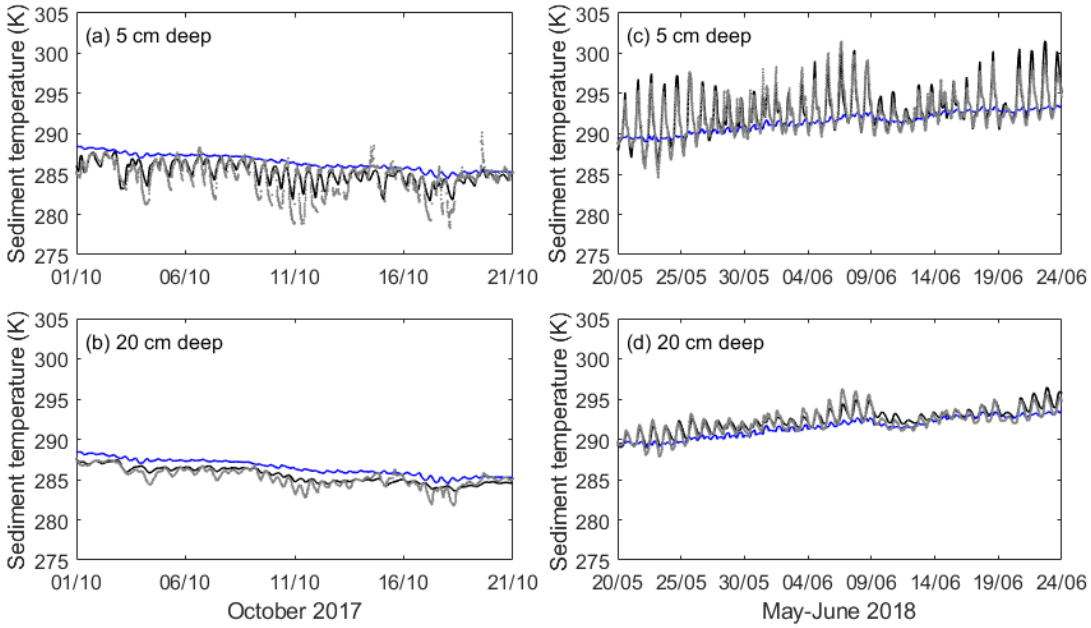

Figure 6: Comparison between the *in situ* sediment temperature measurements (grey dots) and the model output (black line) for October 2017 (a, b) and May-June 2018 (c, d) at 5 cm deep (a, c) and 20 cm deep (b, d) within the sediment using the mean fitted parameters ζ (constant, -), μ (thermal diffusivity, $m^2.s^{-1}$, and η (conductivity, $W.m^{-1}.K^{-1}$) all periods considered (Table 3). The blue line is the water temperature from the Marel Carnot station.

Predicted trends of the sediment temperature variations according to time and space. In general, the sediment temperature reconstructed by the model reproduced the trends of observed air, water temperatures and solar radiation, showing higher temperature in summer and lower temperature in winter at all bathymetric levels (Figs. 7g, h, i). The amplitude of sediment temperature as well as its daily variation was smaller on the infralittoral (mostly driven by the water temperature) compared to the higher foreshore (mostly driven by the air temperature and the other forcing variables) at 5 and 30 cm deep (Fig. 7).

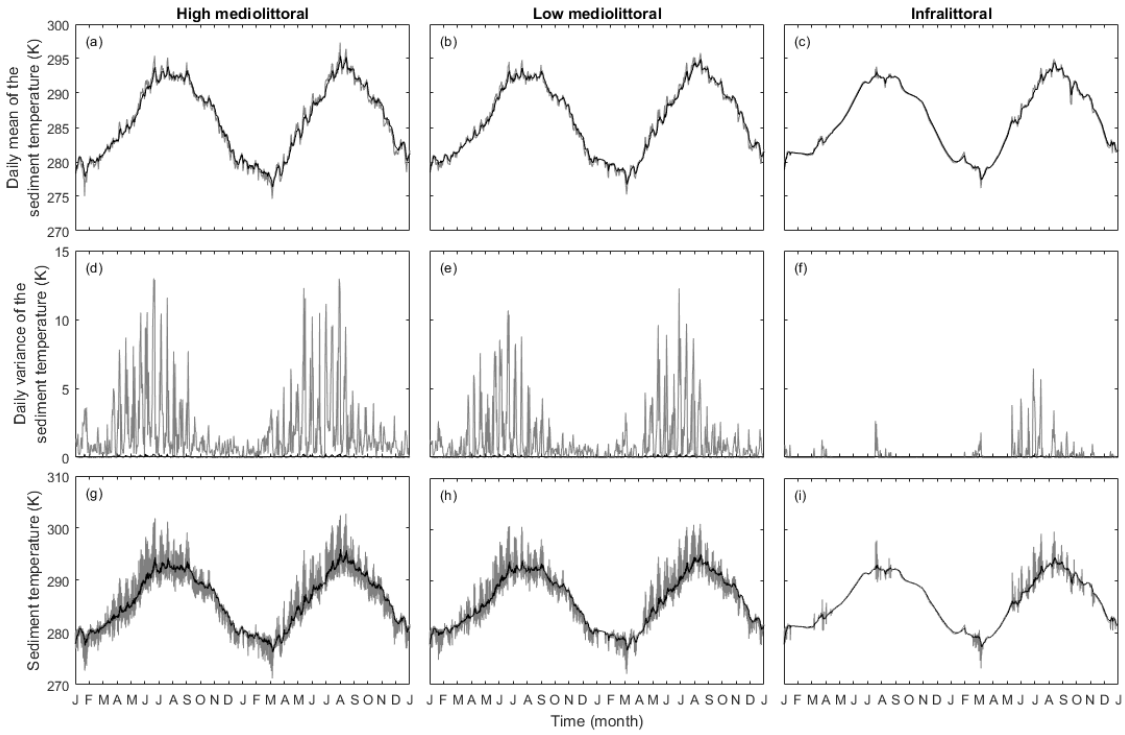

Figure 7: Daily means (a, b, c) and associated variations (d, e, f) of the sediment temperature (g, h, j) predicted by the sediment temperature model implemented in this study at 5 cm deep (grey lines) and 30 cm deep (black lines) on the high mediolittoral shore (a, d, g), the low mediolittoral shore (b, e, h) and the infralittoral shore (c, f, i) at Wimereux (Eastern English Channel, France).

The highest amplitude of sediment temperature variation occurred on the high mediolittoral foreshore at 5 cm deep, with associated daily variation of up to 14 °C in summer time (Figs. 7d, g). At 30 cm deep at the same location, the daily variation of the sediment temperature was close to 0 °C (Fig. 7f).

3.3. Patterns in Arrhenius temperature of Arenicola marina outside its temperature tolerance range

The low and high boundaries of the temperature tolerance range of *A. marina* were estimated to be respectively $T_L = 272.8$ K and $T_H = 297.7$ K. The values of the Arrhenius temperature outside the species' temperature tolerance range were much higher than the Arrhenius temperature within the species' temperature tolerance range ($T_A = 4014$ K), with respectively $T_{AL} = 69080$ K and $T_{AH} = 82380$ K, highlighting a rapid decrease in metabolic activity outside species' temperature tolerance range (Fig. 8).

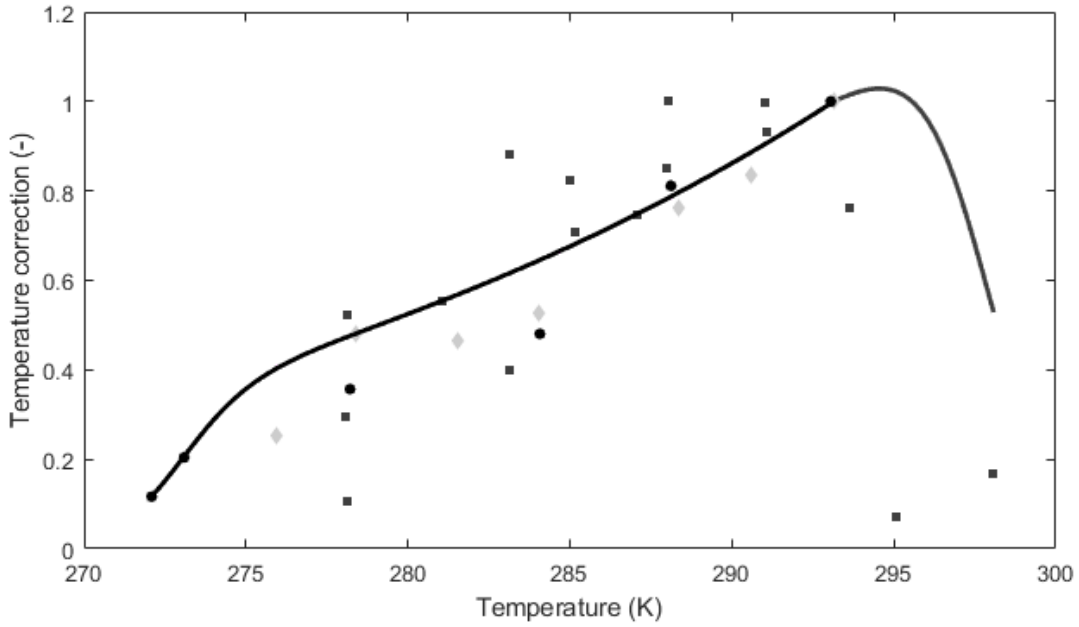

Figure 8: Arrhenius plot (line) obtained by fitting the parameters of an abj-DEB model for *Arenicola marina* as previously performed by De Cubber et al. (2019) with additional dataset consisting in: fertilization success rate data (dark grey squares, Lewis et al., 2002), oxygen consumption rate data (light grey diamonds, Schröer et al., 2009) and mitochondrial respiration rate data (black dots, Sommer and Pörtner, 2004) at several temperatures. The fitted values of the lower and the higher boundary (dashed lines) of the temperature tolerance range are respectively $T_L = 272.8$ K and $T_H = 297.7$ K. The value of the Arrhenius temperature within those boundaries is 4014 K. The fitted value of the Arrhenius temperature before the lower boundary is $T_{AL} = 69080$ K, and after the higher boundary is $T_{AH} = 82380$ K.

The complete parameter set of the updated abj-DEB model for *A. marina* is given in Sup. Mat. 1 to 8. No major changes in the parameters were observed compared to the previous parameter estimation (Sup.Mat.1, to compare with the

parameter set provided by De Cubber et al. (2019)) and slightly better fitness values were obtained with the updated version concerning both the mean relative error MRE (0.22 in the updated version vs. 0.23 in the former version) and the symetric mean squared error SMSE (0.27 vs. 0.28).

3.4. In situ estimated food resources

3.4.1. In situ growth of the recruits

Because of the low number of individuals belonging to the larger trunk length classes from 8 to 12 cm (older individuals) (Fig. 4), the decomposition of the population in different age groups after 2 to 3 years was difficult and only the newest cohorts were followed to reconstruct the *in situ* growth and associated scaled functional response. The growth of the recruits from May 2017 was possible to be followed for one year (from May 2017 to May 2018). The growth of the recruits from May 2018 was estimated only from the end of May to mid July 2018 (Fig. 9, Table 4). The population growth appeared faster between July and September 2017 and between the end of May and mid July 2018, and slower between January and March 2018 (Fig. 9, Table 4).

When considering the contribution of each foreshore level to the cohort followed, it appeared that the recruits were gradually migrating from the high mediolittoral bathymetric level (100 % of the recruits came from this level in May of both years) to the low mediolittoral and infralittoral bathymetric levels (33 to 40 % of the recruits came from the low mediolittoral and 7 to 20 % of the recruits came from the infralittoral bathymetric levels after 10 to 12 months since recruitment) as previously suggested in Fig. 4 (Table 4). The relation between the trunk length (TL, cm) of *A. marina* and the bathymetric level ($bath$, m) could be established as:

$$bath = -0.29 \cdot TL + 6.60 \tag{6}$$

(Linear regression, $R^2 = 0.99$)(Fig. 10). It was used in the prediction scenarios part. Here, it appeared clearly that lugworms were found lower on the foreshore when they had grown larger.

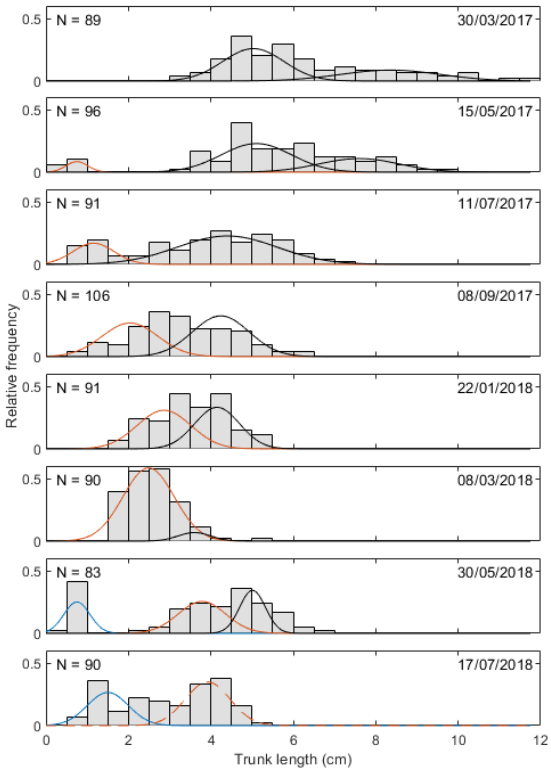

Figure 9: Cohorts decomposition of the population structure of *Arenicola marina* at Wimereux (Eastern English Channel) with a Bhattacharya analysis of the trunk length (TL) frequency distributions (5-mm size class intervals) at 8 sampling dates between March 2017 and July 2018. The histograms represent the relative number of individuals collected belonging to each trunk length class, the lines (orange, black and blue) are the cohorts given by the Bhattacharya analysis. The total number of individuals collected at each date are given on the left corner of each graph (as N = #) and the corresponding dates are given in the right corner of each graph. The orange line represents the trunk length distribution of the recruits cohort of 2017 (the dashed line was not used in further analyses), the blue line represents the trunk length distribution of the recruits cohort of 2018. Their associated mean trunk length and standard error are given in Table 4. The black cohorts given by the Bhattacharya analysis were not used further in the study of the *in situ* growth of the population.

Table 4: Mean trunk lengths (TL) and standard deviation of the recruits cohorts of 2017 and 2018 and associated contributions of each foreshore level to the cohort followed (high = high mediolittoral, medium = low mediolittoral and low = infralittoral).

Date	Recruits 2017				Recruits 2018			
	Mean TL (cm)	High	Medium	Low	Mean TL (cm)	High	Medium	Low
15/05/2017	1.00 ± 0.26	100%	0%	0%	-	-	-	-
11/07/2017	1.40 ± 0.50	80%	20%	0%	-	-	-	-
08/09/2017	2.29 ± 0.68	87%	8%	5%	-	-	-	-
22/01/2018	3.11 ± 0.66	70%	23%	7%	-	-	-	-
08/03/2018	2.74 ± 0.62	41%	33%	27%	-	-	-	-
30/05/2018	4.04 ± 0.58	53%	40%	7%	1.00 ± 0.32	100%	0%	0%
17/07/2018	-	-	-	-	1.75 ± 0.50	85%	15%	0%

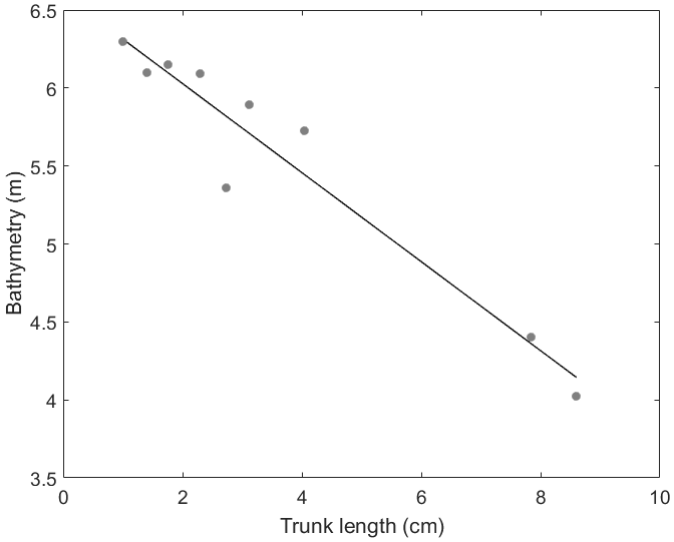

Figure 10: Observations (dots) and linear relation (line) between the trunk length (TL, cm) of *Arenicola marina* at Wimereux (Eastern English Channel) and the mean bathymetric level (*bath*, m) where they were collected (according to Table 4 and Figs. 4 and 9).

390 *3.4.2. Reconstruction of the scaled functional response*

391 The abj-DEB model for *Arenicola marina* associated to the sediment temperature
392 model reconstruction at different depths and bathymetric levels, and the associated
393 Arrhenius temperature correction, enabled a good fit between the predicted and the
394 observed trunk lengths (Fig. 11 a). The reconstructed scaled functional response
395 was lower in the autumn-winter period and higher during the spring-summer period,
396 with values ranging from 0.01 in winter to 0.4 in summer 2017 and up to 0.5-0.6 in
397 spring and summer 2018 (Figs. 11 a, b). In general, these trends were also observed
398 when considering the chlorophyll-a concentration of the seawater (Chla, µg.L^{-1}), with
399 the highest values in spring 2017 and 2018, and between the end of the summer and
400 the beginning of the autumn 2017 (Fig. 11 c). The fitting of the scaled functional
401 response to Chla led to a half-saturation coefficient X_K value of 5.00 µg.L^{-1} of Chla
402 (Fig. 12). The total nitrogen content of sediment (%) showed a spatial pattern
403 with higher nitrogen concentrations on the lower shore level compared to a lower
404 concentration on the higher shore. Besides, the nitrogen concentration on the high
405 mediolittoral shore did not display significant seasonal variations compared to the
406 nitrogen concentration of the infralittoral shore (Fig. 11 c).

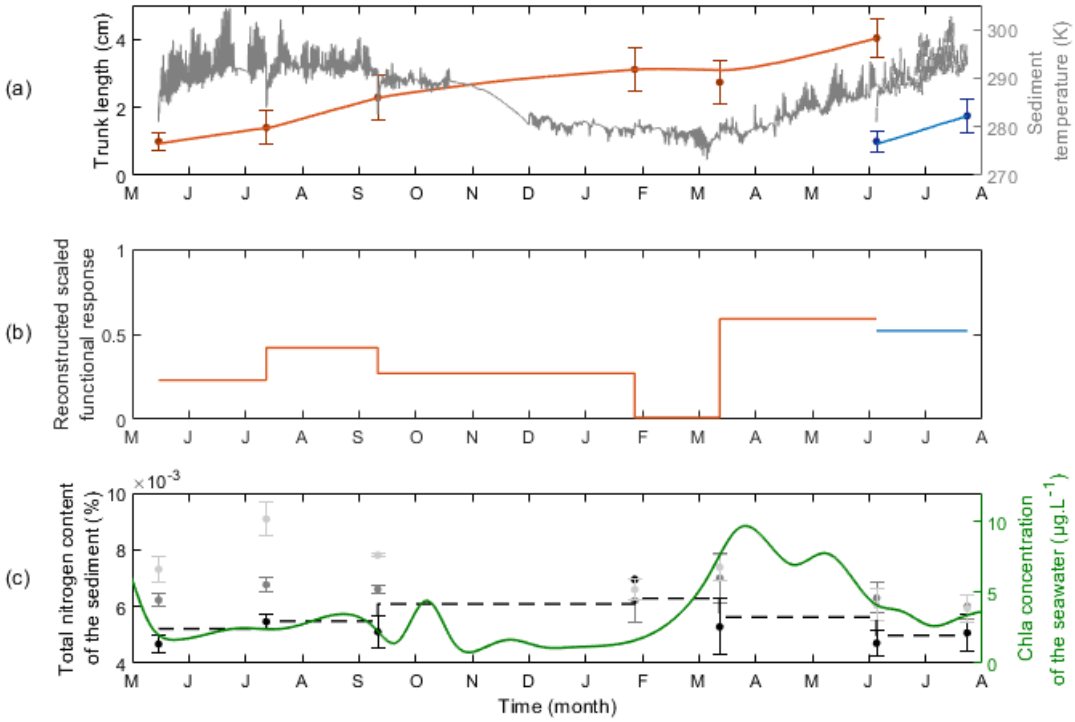

Figure 11: Reconstruction of the scaled functional response values (b) by fitting the predicted trunk length growth from a Dynamic Energy Budget model for *Arenicola marina* (red and blue lines) to the trunk length (cm) growth observations (red and blue dots) using the Arrhenius temperature (a) (Equation (3), Fig. 8) of the sediment temperature (K) reconstruction (grey line) according to the sediment temperature model as well as depth and the bathymetric level (a) and associated levels of the total nitrogen content of sediment (%) on the high, low mediolittoral and infralittoral bathymetric levels (dots, respectively in black, dark and light grey) and experienced by the recruits (dashed line) as well as the associated concentration in chlorophyll-a of the seawater (µg.L^{-1}) (green line, SOMLIT data) (c).

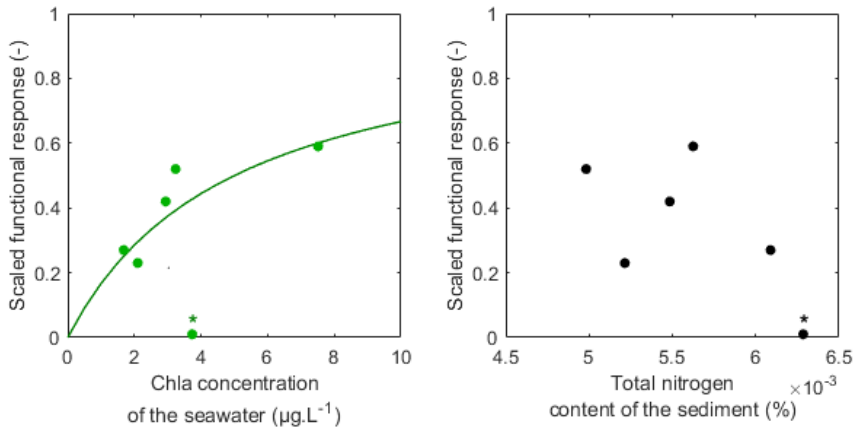

Figure 12: Reconstructed scaled functional response according to (left) chlorophyll-a concentration (µg.L^{-1}) (green dots) and associated fitted response $f = Chla/(Chla + X_K)$ (green line, $X_K = 5.00$ µg.L^{-1}) and (right) total nitrogen content of sediment reconstructed from the observations of nitrogen content of sediment on the different levels of the beach and the contribution of each bathymetric level to the recruits cohorts (Fig. 11, Table 4). The dots with asterisk were not used for the fitting (other mechanisms such as migration might be implied).

However, although the nitrogen content trend of the infralittoral seem to be correlated with the reconstructed scaled functional value, there was no clear relation between the reconstructed scaled functional response and the nitrogen content of the sediment in which lugworms live (Fig. 12).

3.5. Bathymetric level and depth effects on growth and reproduction

The different migration scenarios induced different temperature patterns experienced by lugworms (Fig. 13). As expected, the lugworms remaining on the high mediolittoral shore in superficial galleries (light grey scenario) experienced the most extreme daily temperatures, especially in summer and winter time, with temperature variations between the sediment and the seawater reaching up to 14 °C in summer time and 8 °C in winter time (Fig. 13).

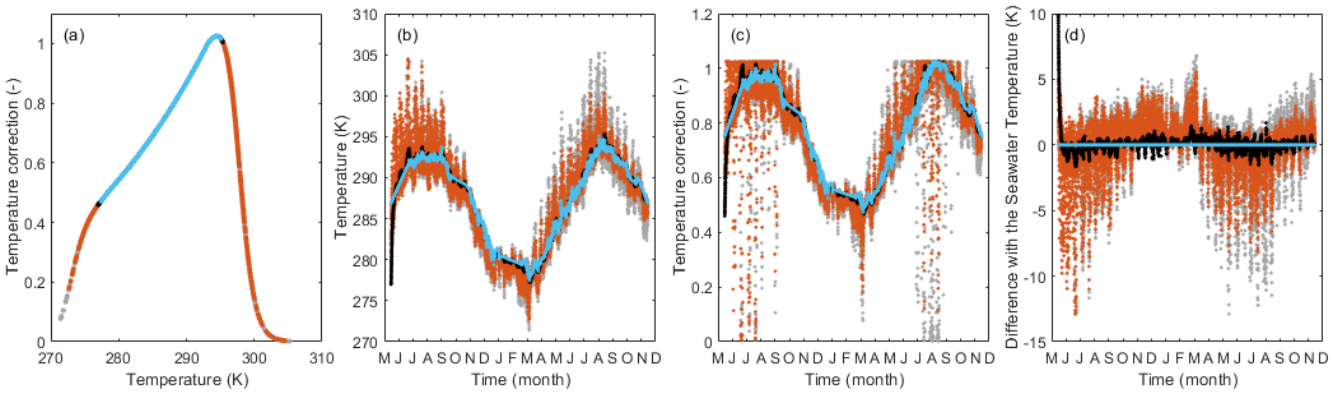

Figure 13: Comparison of temperatures and temperature corrections associated to different migrations scenarios to water temperature. Distribution of temperature corrections associated to different migration scenarios according to temperature (a) and the period of the year (c), sediment temperature corresponding to the different scenarios and seawater temperature according to the period of the year (b) and difference between seawater temperature and sediment temperature of the different scenarios according to the period of the year (d). Blue dots correspond to the seawater temperature. Black dots correspond to the sediment temperature experienced by the lugworms remaining on the infralittoral shore level and buried at 30 cm deep, light grey dots to sediment temperature experienced by the lugworms remaining on the high mediolittoral shore level and buried at 5 cm deep. Red dots correspond to the sediment temperature experienced by the lugworms migrating down the shore and gradually burying deeper in the sediment.

The lugworms remaining on the infralittoral shore in deep galleries experience the least extreme daily temperatures (black scenario), with temperature variations between the sediment and the seawater rarely reaching more than 2 °C (Fig. 13).

The lugworms migrating and digging deeper galleries experienced intermediate temperatures in between these two extremes, gradually getting closer to the deep and infralittoral sediment temperature. However, differences with the seawater temperature are still high after one year in both horizontal and vertical migrations, still reaching up to 8 °C in summer and 3 °C in winter (Fig. 13). Nonetheless, the temperature effect on growth and egg production, was minimal compared to the effect of food limitation on the higher shore (Fig. 14).

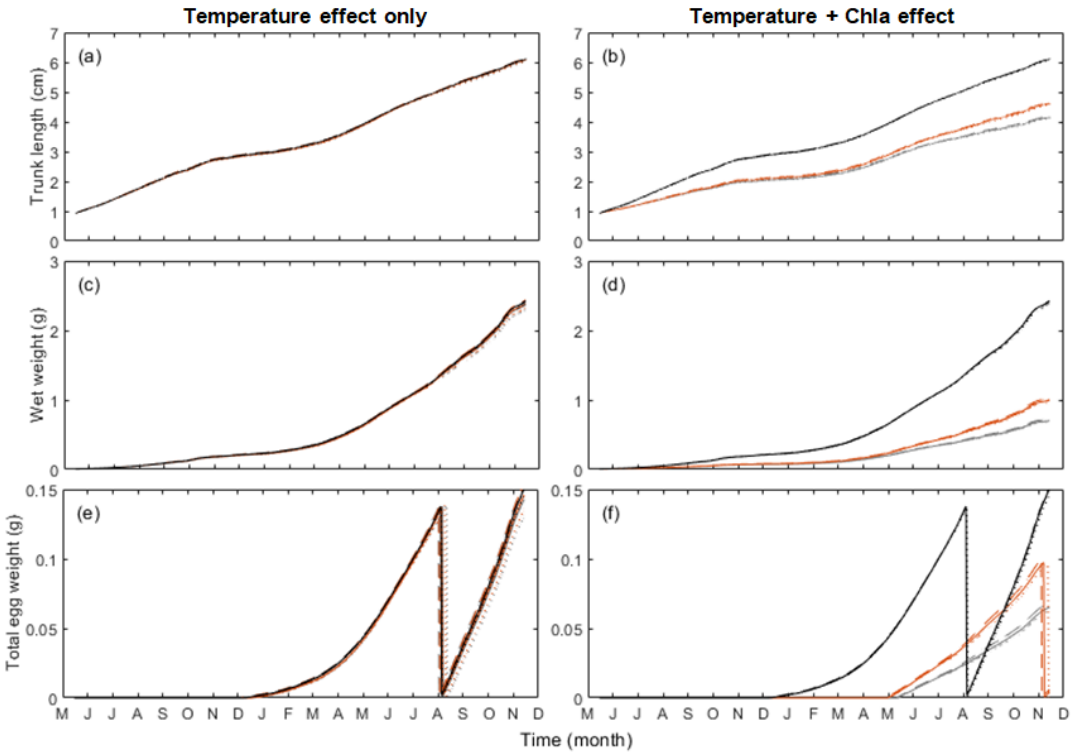

Figure 14: Evolution of the predicted (lines) trunk length (cm) (a,b), wet weight (g) (c,d) and egg weight (g) (e,f) of *Arenicola marina* at Wimereux (Eastern English Channel) according to the period of the year when considering that the food level was the same everywhere (temperature effect only) (a,c,e) or that the food level on the higher shore was half of the food level on the lower shore (b,d,f). The light grey lines correspond to the scenarios where lugworms remain on the high mediolittoral shore, the black lines to the scenarios where lugworms remain on the infralittoral shore, and the orange lines the scenarios where lugworms migrate down the shore. Dashed lines correspond to lugworms staying in 30 cm deep galleries, dotted lines to lugworms staying in 5 cm deep galleries and plain lines to lugworms digging deeper galleries when growing according to Equation (4).

Indeed, when considering that the food level was the same everywhere on the foreshore, growth and egg production differences between scenarios were barely no-

ticeable (Figs. 14 a,c,e). When considering that the food level on the higher shore was half of the food level on the lower shore, the growth was much higher on the lower shore than on the higher shore, even allowing an earlier spawning event in August (Figs. 14 b,d,f).

4. Discussion

4.1. Sediment temperature and metabolic response to temperature

The model output of the sediment temperature model fits to the observations of May-June 2018. However, the ajustment is not as good when considering the data of October 2017. This could be linked to a higher hydrodynamism at this period of the year and the subsequent sediment reworking leading to a displacement of the temperature probes in its vertical position towards the surface within the sediment (higher wind speed, see Fig. 2). The estimated parameter values of η and μ ($\eta = 3.32$ W.m^{-1}.K^{-1} and $\mu = 5.02e^{-7}$ m^2.s^{-1}) for the sand habitat in this study are 4 times higher and almost equal respectively to the ones presented by Guarini et al. (1997) and Savelli et al. (2018) ($\eta = 0.8$ W.m^{-1}.K^{-1} and $\mu = 4.8e^{-7}$ m^2.s^{-1}) for a mud habitat. However, the value of η given in this study ($\eta = 3.32$ W.m^{-1}.K^{-1}) is close to the value of the thermal conductivity of the saturated medium sand according to Hamdhan and Clarke (2010), who measured $\eta = 3.34$ W.m^{-1}.K^{-1}. The estimated value of ζ ($\zeta = 1.21$) lies in the range of what was estimated by Guarini et al. (1997) and Savelli et al. (2018), with respectively $\zeta = 1$ in Savelli et al. (2018) and $\zeta = 1.68$ in Garini et al. (1997). Improvements of the temperature recording set up such as the fixation of a metal rod to large rocks embedded within the sediment and the daily depth follow-up of the probes could be considered to refine the estimated parameters.

The body temperature of lugworms might also be different from the temperature of the surrounding environment, even in ectotherms (Kearney et al., 2008; Porter et al., 1973; Smith et al., 2016). Indeed, Kearney et al. (2008) predicted discrepancies of up to 5 - 6 °C between body and air temperature for cane toad individuals in Australia using the equation of the standard steady state energy balance: $Q_{solar} + Q_{IRin} + Q_{metab} + Q_{conv} + Q_{cond} = Q_{resp} + Q_{evap} + Q_{IRout}$. In the case of

marine benthic organisms, dug in a sediment saturated in water and not exposed to solar radiations, the main energy flux driving the body temperature must be the conduction flux from the sediment, depending on the surface/volume ratio of the individual, leading to higher thermal inertia in larger individuals. The fluxes linked to solar radiation, respiration, convection and evaporation, which are the more likely to induce discrepancies between the body temperature and the environment temperature in terrestrial environments (Kearney et al., 2008), can be neglected in the present study. However, on the high mediolittoral part of the shore mainly, the drying of the surface sediment during the long emersion periods, in addition of causing anaerobic stress, could lead to unsaturated sediments and increase the evaporation flux. It might also accentuate the extreme sand temperatures causing higher stress to the recruits present on this level and should be taken into account in further studies.

The re-estimation of the Arrhenius temperature within the species temperature tolerance range boundaries T_A ($T_A = 4014$ K) lead to a value close to the previous estimation ($T_A = 3800$ K) (De Cubber et al. (2019). The Arrhenius temperatures at lower ($T_{AL} = 69080$ K) and upper ($T_{AH} = 82380$ K) limits of the species tolerance range are overall close to what was observed by Monaco and McQuaid (2018) for *Mytilus galloprovincialis* and *Perna perna*, two species of bivalves living on the intertidal rocky shore, with T_{AL} respectively ranging from 22670 K to 55400 K and T_{AH} respectively ranging from 34540 K to 250600 K. The higher boundaries of the two species tolerance range were higher than the one estimated for *A. marina* (297.7 K) with values of 309 K for *Perna perna*, and 306.1 K for *Mytilus galloprovincialis*, which was to be expected given their distribution in warmer waters (Mediterranean, subtropical and tropical areas). The lower boundaries of the two species tolerance range were close to the one estimated for *A. marina* (272.8 K) with respective values of 273 K for *Perna perna*, and 279.6 K for *Mytilus galloprovincialis*. These values are important to understand the possible climate migration enhancing new geographical distribution of marine species due to global warming, as done by Thomas and Bacher (2018) with three European marine bivalve species.

4.2. Food level reconstruction and scaled functional response

The reconstructed scaled functional response range of this study appears in accordance with the annual mean value previously estimated around 0.4 at the same site during approximately the same period (De Cubber et al., 2019). The increase of the total nitrogen content of sediment when going down the shore seems consistent with the shorter emersion periods met there. The organic nitrogen content of sediment from the shore could come from various sources of primary producers (microphytobenthos (MPB), deposited phytoplankton, macroalgae in decomposition, bacteria...) (Gaudron et al., 2016). The absence of correlation between the evolution of nitrogen content of sediment and the scaled functional response found in this study might be due to the evolution of the contribution of non- or less-assimilated nitrogen sources to the total nitrogen content such as macroalgae debris to the total nitrogen of the sediment. Indeed, lugworms are supposed to feed mainly on MPB and bacteria but are almost unable to digest macro debris (Andresen and Kristensen, 2002; Retraubun et al., 1996; Rikjen, 1979). The high hydrodynamism during winter periods could bring more debris leading to higher nitrogen contents of the sediment than what the scaled functional response seems to point out because of their potential low digestibility.

However, the scaled functional response was quite well correlated to the chlorophyll-a concentration of the seawater. This could be part of the food source contribution to the lugworms diet at their early life-stages as it is known that there is a a strong bentho-pelagic trophic coupling between benthic species and pelagic sources in some coastal habitats. Indeed, phytoplankton was also reported in lugworms diet on the East Coast of the Cotentin Peninsula (English Channel, Normandy, France) (Gaudron et al., 2016). The correlation with the chlorophyll-a concentration of the seawater could also be explained by the fact that the food sources (MPB and bacteria) show in average similar growth and production patterns than phytoplankton (Lefebvre et al., 2009).Therefore, chlophyll-a concentration is a good proxy to estimate the level of food in the lugworms' diet.

Besides, the estimation of the scaled functional response from the observation of cohort growth instead of individual growth might show some limitations. In-

deed, other population processes such as migration (between February and March 2018) or on-going recruitment (between May and July 2017) might have lead to some under- or over-estimation of the growth and the associated scaled functional response. Moreover, the assessment of the scaled functional response and its associated food proxy might be site-dependent to some extent, and our results should therefore be taken with caution when considering different locations. Indeed, food sources might vary among sites, potentially leading to different scaled functional responses for the same food proxy (Chla in our study) since the latter is not the only component of lugworms' diet. Nonetheless, we believe that our study site is similar to many other sandy beaches described as inhabited by lugworms and only small variations of the half-saturation coefficient (linked to the assimilation of food) might occur. Further studies on *in situ* sources of food and the link between food sources and scaled functional response are needed. Besides, other proxies for food such as benthic chlorophyll-a might be interesting to explore.

4.3. Growth scenarios

The trunk length and wet weight growth as well as the total egg weight were not really influenced by the temperature changes along the shore. However, the increase of food levels down the shore induced higher wet weight and trunk length growth as well as a higher total egg weight, and lead to an earlier first spawning event, suggesting that lugworms migrate down the shore to get access to more food rather than avoiding extreme temperatures. Since individuals recruiting down the shore experience higher growth, the recruitment location on the higher shore might be linked to other constraints such as the fact that juveniles can not swim against the tide current, or to intraspecific competition for food and space with juveniles avoiding the adults grounds as already suggested by several authors, or to avoid predation (De Vlas, 1979; Farke et al., 1979; Flach and Beukema, 1994).

A number of active movement behaviours to avoid whether cold or warm extreme temperatures have already been documented both in terrestrial and marine species, among which digging (Fitzpatrick et al., 2019; Kearney et al., 2009; Kolbe et al., 2010) or moving to sheltered places (Chapperon and Seuront, 2011; Kearney et al., 2009; Malishev et al., 2017; Monaco et al., 2016). In *A. marina*, shore migrations

due to extreme cold temperatures (below 0 °C) have already been reported by Reise et al. (2001) but the depth at which the galleries of lugworms was dug into was not considered. In the present study, the down-shore migration of *A. marina* recruits started quite early (in July) but with a slight acceleration of the process between January and March. Although this is when the coldest sediment temperature of the year was recorded, given the low response of growth and egg production to temperature variations, other clues might explain a migration at this period of the year. Extreme temperatures (whether warm in July or cold in January) might indeed not be the actual trigger of the down-shore migrations of lugworms. However, the increase of primary production at this period of the year might induce lugworms to migrate down the shore.

Although the effect of temperature alone seems limited, other parameters, such as the desiccation of the superficial sediment at low tide, could, if taken into account, change this observation increasing the variability of temperature and the subsequent occurrence of extreme temperatures. Moreover, the potential hypoxia experienced by lugworms at low tide was not considered, although hypoxic metabolic activity has been reported by several authors for this species (Schöttler et al., 1984), and hypoxia was shown to impact growth and reproduction in marine bivalves (Aguirre-Velarde et al., 2019). As lower levels of the shore are emerged on shorter periods and deeper galleries give access to interstitial water within the sediment (Shumway and Davenport, 1977), this parameter should also be explored to explain the down-shore migrations of *A. marina*. Indeed, the oxygen consumption of lugworms decreases with oxygen saturation (Shumway, 1979), leading to a possible change in metabolic activity. As an example, if we compare the oxygen consumption of 1 g and 6 g lugworms respectively at 12 °C and 20 °C to the oxygen quantity contained in oxygen-saturated seawater, it appears that smaller lugworms consume 20 % of the oxygen in 15 to 30 hours while larger lugworms consume the same quantity in only 3.8 to 8.5 hours (considering lugworm densities are not too high). At low tide, large lugworms on the higher mediolittoral shore (where emersion periods are longer and water renewal is lower) might have a decrease in their metabolic activity linked to a depletion in dissolved oxygen concentration within the sediment. This effect might

be amplified when temperatures above 25 °C are reached, potentially explaining why lugworms migrate downwards on the shore. For larger individuals (rarely found on the higher shore), food concentration might therefore not be the only trigger for down-shore migration and might be the result of several interplaying variables. To account for this reduction of metabolic activity of adults at low tide, an extra parameter combined to the temperature correction could be computed according to the shore level and the depth of the gallery as previously explored by Monaco and McQuaid (2018) in two intertidal bivalve species.

4.4. Management perspectives

The present study constitutes a valuable first step to better understand the effects of temperature on juvenile and adult populations of *Arenicola marina* such as their small-scale migration behaviour once recruited in a temperate ecosystem.

Between March 2017 and July 2018, most lugworms larger than 7 cm disappeared, traducing the disappearance of older individuals. The disappearance of the largest age classes coincided with the presence of higher number of fishermen in summer 2017 on the study site (pers. observation). De Cubber et al. (2018) has shown the need for some regulation on *Arenicola* spp. fisheries for some areas of the Eastern English Channel based on the density of individuals. The study of the population structure might also be another criteria to decide on the need to implement relevant management measures.

Besides, this study opens new insights on the migration of the lugworms within a population showing the typical distribution pattern, as well as tools to model populations *in situ* growth and reproduction. This could prove useful for management purposes to test scenarios for the prediction of spawning events (Pecquerie et al., 2009; Watson et al., 2000) or predict *in situ* lengths at puberty or harvest sizes and where these lengths are found on the shore. These models could then be associated to individual-based model and larval dispersal models in order to better understand the population dynamics and connectivity of the species (Bacher and Gangnery, 2006; Martin et al., 2012; Nicolle et al., 2017) which would also prove useful for conservation managers.

The knowledge of environmental conditions, behavioural and metabolic responses

of the organism to those and DEB models has also been used to model ecological niches (Kearney et al., 2010; Thomas and Bacher, 2018). Modelling the ecological niche of *A. marina* could help to estimate the impact of fisheries on the species by comparing the species potential distribution with the current species distribution. An ecological niche model could also enable to make predictions on the effect of global change on the species distribution (Thomas and Bacher, 2018) and the possible related impact on other key species. As an example, *A. marina* has been shown to impact negatively populations of *Zostera noltii* (Kosche, 2007) and to influence the local community compositions (Donadi et al., 2015). Its expansion in southern areas (suggested by Pires et al., 2015) might lead to shift in species communities in these areas.

5. Conclusions

In the present study, we have successfully identified and simulated relevant environmental variables needed for the implementation of a DEB model for *Arenicola marina*, as well as their spatial variations along the foreshore. Combining the characterization of the down-shore migration of a local population of *A. marina* with these environmental variables as inputs for the DEB model, we were able to discard the hypothesis that temperature constituted the main trigger for lugworm migration. The increase of food level when migrating down the shore seems to account for an important trigger, but other potential temperature-related factors such as desiccation and hypoxia should also be explored in future studies. The present study could prove usefull for conservation managers *per se* when defining relevant management measures linked to lugworm individual life-traits. Besides, the association of the present DEB model to further population dynamics models will permit a complete management plan for *A. marina* populations.

Acknowledgements

We would like to thank V. Cornille for his technical support on the field and G. Watson for his precious advice on *in situ* temperature probes deployment. This work was partly funded by the University of Lille and CNRS. We are grateful to Europe

(FEDER), the state and the Region Hauts-de-France for funding the experimental set up and T. Lancelot (research assistant) through the CPER MARCO 2015 - 2020. L. De Cubber was funded by a PhD studentship from the University of Lille and a post-doctoral fellowship through the CPER MARCO.

References

Aguirre-Velarde, A., Thouzeau, G., Jean, F., Mendo, J., Cueto-Vega, R., Kawazo-Delgado, M., Vásquez-Spencer, J., Herrera-Sanchez, D., Vega-Espinoza, A., Flye-Sainte-Marie, J., 2019. Chronic and severe hypoxic conditions in Paracas Bay, Pisco, Peru: Consequences on scallop growth, reproduction, and survival. Aquaculture, 512: 734259. https://doi.org/10.1016/j.aquaculture.2019.734259

Andresen, M., Kristensen, E., 2002. The importance of bacteria and microalgae in the diet of the deposit-feeding polychaete *Arenicola marina*. Ophelia, 56: 179–196. https://doi.org/10.10 80/00785236.2002.10409498

Bacher, C., Gangnery, A., 2006. Use of dynamic energy budget and individual based models to simulate the dynamics of cultivated oyster populations. Journal of Sea Research, 56: 140–155.

van Bavel, C.H.M., Hillel, D.I., 1976. Calculating potential and actual evaporation from a bare soil surface by simulation of concurrent flow of water and heat. Journal of Agricultural Meteorology, 17: 453–476.

Beukema, J.J., 1995. Long-term effects of mechanical harvesting of lugworms *Arenicola marina* on the zoobenthic community of a tidal flat in the Wadden Sea. Netherlands Journal of Sea Research, 33: 219–227. https://doi.org/10.1016/0077-7579(95)90008-X

Beukema, J.J., De Vlas, J., 1979. Population parameters of the lugworm *Arenicola marina* living on tidal flats in the Dutch Wadden Sea. Netherlands Journal of Sea Research, 13: 331–353. https://doi.org/10.1016/0077-7579(79)90010-3

671 Brock, T.D., 1981. Calculating solar radiation for ecological studies. Ecologi-
672 cal Modelling, 14: 1-19.

673 Cadman, P.S., 1997. Distribution of two species of lugworm (*Arenicola*) (An-
674 nelida: Polychaeta) in South Wales. Journal of the Marine Biological Associ-
675 ation of the U.K., 77: 389–398. https://doi.org/10.1017/S0025315400071745

676 Chapperon, C., Seuront, L., 2011. Space–time variability in environmental
677 thermal properties and snail thermoregulatory behaviour. Functional Ecology,
678 25: 1040–1050. https://doi.org/10.1111/j.1365-2435.2011.01859.x

679 Clarke, L.J., Hughes, K.M., Esteves, L.S., Herbert, R.J.H., Stillman, R.A.,
680 2017. Intertidal invertebrate harvesting: a meta-analysis of impacts and re-
681 covery in an important waterbird prey resource. Marine Ecology Progress
682 Series, 584: 229–244. https://doi. org/10.3354/meps12349

683 De Cubber, L., Lefebvre, S., Lancelot, T., Denis, L., Gaudron, S.M., 2019.
684 Annelid polychaetes experience metabolic acceleration as other Lophotrocho-
685 zoans: inferences on the life cycle of *Arenicola marina* with a Dynamic Energy
686 Budget model. Ecological Modelling, 411: 108773.

687 De Cubber, L., Lefebvre, S., Fisseau, C., Cornille, V., Gaudron, S.M., 2018.
688 Linking life-history traits, spatial distribution and abundance of two species of
689 lugworms to bait collection: A case study for sustainable management plan.
690 Marine Environmental Research, 140: 433-443. https://doi.org/10.1016/ j.mar
691 envres.2018.07.009

692 De Vlas, J., 1979. Secondary production by tail regeneration in a tidal flat
693 population of lugworms (*Arenicola marina*), cropped by flatfish. Nether-
694 lands Journal of Sea Research, 13: 362–393. https://doi.org/10.1016/0077-
695 7579(79)90012-7

696 De Wilde, P.A.W.J., Berghuis, E.M., 1979. Laboratory experiments on growth
697 of juvenile lugworms, *Arenicola marina*. Netherlands Journal of Sea Research,
698 13: 487–502. https://doi.org/10.1016/ 0077-7579(79)90020-6

699 Donadi, S., van der Heide, T., Piersma, T., van der Zee, E.M., Weerman,
700 E.J., van de Koppel, J., Olff, H., Devine, C., Hernawan, U.E., Boers, M.,
701 Planthof, L., Klemens Eriksson, B., 2015. Multi-scale habitat modification
702 by coexisting ecosystem engineers drives spatial separation of macrobenthic
703 functional groups. Oikos, 124: 1502–1510. https://doi.org/10.1111/oik.02100

704 Farke, H., Berghuis, E.M., 1979a. Spawning, larval development and migra-
705 tion of *Arenicola marina* under field conditions in the western Wadden sea.
706 Netherlands Journal of Sea Research, 13: 529–535.

707 Farke, H., Berghuis, E.M., 1979b. Spawning, larval development and migration
708 behaviour of *Arenicola marina* in the laboratory. Netherlands Journal of Sea
709 Research, 13: 512–528.

710 Farke, H., de Wilde, P.A.W.J., Berghuis, E.M., 1979. Distribution of juvenile
711 and adult *Arenicola marina* on a tidal mud flat and the importance of nearshore
712 areas for recruitment. Netherlands Journal of Sea Research, 13: 354–361.
713 https://doi.org/10.1016/0077-7579(79)90011-5

714 Fitzpatrick, M.J., Zuckerberg, B., Pauli, J.N., Kearney, M.R., Thompson,
715 K.L., Werner II, L.C., Porter, W.P., 2019. Modeling the distribution of niche
716 space and risk for a freeze-tolerant ectotherm, *Lithobates sylvaticus*. Eco-
717 sphere, 10: 1–19. https://doi.org/10.1002/ecs2.2788

718 Flach, E.C., Beukema, J.J., 1994. Density-governing mechanisms in popula-
719 tions of the lugworm *Arenicola marina* on tidal flats. Marine Ecology Progress
720 Series, 115: 139–150. https://doi.org/ 10.3354/meps115139

721 Gaudron, S.M., Grangeré, K., Lefebvre, S., 2016. The comparison of δ13C
722 values of a deposit- and a suspension-feeder bio-indicates benthic vs. pelagic
723 couplings and trophic status in contrasted coastal ecosystems. Estuaries and
724 Coasts, 39: 731–741. https://doi.org/10.1007/s12237-015-0020-x

725 Guarini, J.-M., Blanchard, G.F., Gros, P., Harrison, S.J., 1997. Modelling the
726 mud surface temperature on intertidal flats to investigate the spatio-temporal

dynamics of the benthic microalgal photosynthetic capacity. Marine Ecology Progress Series, 153: 25–36.

Hamdhan, I.N., Clarke, B.G., 2010. Determination of Thermal Conductivity of Coarse and Fine Sand Soils, Proceedings of the World Geothermal Congress.

Kearney, M., Phillips, B.L., Tracy, C.R., Christian, K.A., Betts, G., Porter, W.P., 2008. Modelling species distributions without using species distributions: the cane toad in Australia under current and future climates. Ecography, 31: 423–434. https://doi.org/10.1111/j.0906-7590.2008.05457.x

Kearney, M., Shine, R., Porter, W.P., 2009. The potential for behavioral thermoregulation to buffer 'cold-blooded' animals against climate warming. PNAS, 106: 3835–3840.

Kearney, M., Simpson, S.J., Raubenheimer, D., Helmuth, B., 2010. Modelling the ecological niche from functional traits. Philosophical Transaction of the Royal Society of London Series B, Biological Sciences, 365: 3469–3483. https://doi.org/10.1098/rstb.2010.0034

Kish, N.E., Helmuth, B., Wethey, D.S., 2016. Physiologically grounded metrics of model skill: a case study estimating heat stress in intertidal populations. Conservation Physiology, 4: 1–19. https://doi.org/10.1093/conphys/cow038

Kolbe, J., Kearney, M., Shine, R., 2010. Modeling the consequences of thermal trait variation for the cane toad invasion of Australia. Ecological Applications, 20: 2273–2285. https://doi.org/10.2307/29779619

Kooijman, S.A.L.M., 2010. Dynamic energy budget theory for metabolic organisation. Cambridge University Press, 514 pp.

Kooijman, S.A.L.M., 2006. Pseudo-faeces production in bivalves. Journal of Sea Research, 56: 103–106. https://doi.org/10.1016/j.seares.2006.03.003

Kosche, K., 2007. The influence of current velocity, tidal height and the lugworm *Arenicola marina* on two species of seagrass, *Zostera marina* L. and *Z. noltii* Hornemann. Bremen University.

Kristensen, E., 2001. Impact of polychaetes (*Nereis* spp. and *Arenicola marina*) on carbon biogeochemistry in coastal marine sediments. Geochemical Transactions, 2: 92–103. https://doi.org/10.1186/1467-4866-2-92

Lavaud, R., Flye-Sainte-Marie, J., Jean, F., Emmery, A., Strand, Ø., Kooijman, S.A.L.M., 2014. Feeding and energetics of the great scallop, *Pecten maximus*, through a DEB model. Journal of Sea Research, 94: 5–18. https://doi.org/10.1016/j.seares.2013.10.011

Lefebvre, S., Marín Leal, J.C., Dubois, S., Orvain, F., Blin, J.L., Bataillé, M.P., Ourry, A., Galois, R., 2009. Seasonal dynamics of trophic relationships among co-occurring suspension-feeders in two shellfish culture dominated ecosystems. Estuarine, Coastal and Shelf Science, 82: 415–425. https://doi.org/10.1016/j.ecss.2009.02.002

Lewis, C., Olive, P.J., Bentley, M.G., Watson, G., 2002. Does seasonal reproduction occur at the optimal time for fertilization in the polychaetes *Arenicola marina* L. and *Nereis virens* Sars? Invertebrate Reproduction and Development, 41: 61–71. https://doi.org/10.1080/079 24259.2002.9652736

Longbottom, M.R., 1970. The distribution of *Arenicola marina* (L.) with particular reference to the effects of particle size and organic matter of the sediments. Journal of Experimental Marine Biology a Ecol. 5, 138–157. https://doi.org/10.1016/0022-0981(70)90013-4

Malishev, M., Bull, M.C., Kearney, M.R., 2017. An individual-based model of ectotherm movement integrating metabolic and microclimatic constraints. Methods in Ecology and Evolution, 9: 472–489. https://doi.org/10.1111/ijlh.12426

Martin, B.T., Zimmer, E.I., Grimm, V., Jager, T., 2012. Dynamic Energy Budget theory meets individual-based modelling: A generic and accessible implementation. Methods in Ecology and Evolution, 3: 445–449. https://doi.org/10.1111/j.2041-210X.2011.00168.x

783 Migne, A., Spilmont, N., Davoult, D., 2004. *In situ* measurements of benthic
784 primary production during emersion: Seasonal variations and annual produc-
785 tion in the Bay of Somme (eastern English Channel, France). Continental
786 Shelf Research, 24: 1437–1449. https://doi.org/10.1016/j.csr.2004.06.002

787 Monaco, C.J., McQuaid, C.D., 2018. Applicability of Dynamic Energy Budget
788 (DEB) models across steep environmental gradients. Scientific Reports, 8:
789 16384. https://doi.org/10.1038/s41598-018-34786-w

790 Monaco, C.J., Wethey, D.S., Helmuth, B., 2016. Thermal sensitivity and the
791 role of behavior in driving an intertidal predator-prey interaction. Ecological
792 Monographs, 86: 429–447. https://doi.org/10.1002/ecm.1230

793 Newell, G.E., 1949. The later larval life of *Arenicola marina*. Journal of the
794 Marine Biological Association of the U.K., 28: 635–639. https://doi.org/10.10
795 17/S0025315400023456

796 Newell, G.E., 1948. A contribution to our knowledge of the life history of
797 *Arenicola marina* L. Journal of the Marine Biological Association of the U.K.,
798 27: 554–580. https://doi.org/10.1017/S0025315400056022

799 Nicolle, A., Moitié, R., Ogor, J., Dumas, F., Foveau, A., Foucher, E., Thiébaut,
800 E., 2017. Modelling larval dispersal of *Pecten maximus* in the English Channel:
801 a tool for the spatial management of the stocks. ICES Journal of Marine
802 Science, 74: 1812–1825. https://doi.org/10.1093/icesjms/fsw207

803 Olive, P.J.W., 1993. Management of the exploitation of the lugworm *Areni-*
804 *cola marina* and the ragworm *Nereis virens* (Polychaeta) in conservation ar-
805 eas. Aquatic Conservation: Marine and Freshwater Ecosystems, 3: 1–24.
806 https://doi.org/10.1002/aqc.3270030102

807 Pecquerie, L., Petitgas, P., Kooijman, S.A.L.M., 2009. Modeling fish growth
808 and reproduction in the context of the Dynamic Energy Budget theory to
809 predict environmental impact on anchovy spawning duration. Journal of Sea
810 Research, 62: 93–105. https://doi.org/10.1016/j.seares.2009.06.002

Pires, A., Martins, R., Magalhães, L., Soares, A., Figueira, E., Quintino, V., Rodrigues, A., Freitas, R., 2015. Expansion of lugworms towards southern European habitats and their identification using combined ecological, morphological and genetic approaches. Marine Ecology Progress Series, 533: 177–190. https://doi.org/10.3354/meps11315

Porter, W.P., Beckman, W.A., Dewitt, C.B., 1973. Behavioral implications of mechanistic ecology. Thermal and behavioral modeling of desert. Oecologia 13, 1–54. https://doi.org/10.1007/BF00379617

Rauch, M., Denis, L., 2008. Spatio-temporal variability in benthic mineralization processes in the eastern English Channel. Biogeochemistry, 89: 163–180. https://doi.org/10.1007/s10533-008-9191-x

Reise, K., 1985. Tidal flat ecology - An experimental approach to species interactions, Ecological Studies, 54: 191 pp.

Reise, K., Simon, M., Herre, E., 2001. Density-dependent recruitment after winter disturbance on tidal flats by the lugworm *Arenicola marina*. Helgoland Marine Research, 55: 161–165. https://doi.org/10.1007/s101520100076

Retraubun, A.S.W., Dawson, M., Evans, S.M., 1996. The role of the burrow funnel in feeding processes in the lugworm *Arenicola marina* (L.). Journal of Experimental Marine Biology and Ecology, 202: 107–118. https://doi.org/10.1016/0022-0981(96)00017-2

Rijken, M., 1979. Food and food uptake in *Arenicola marina*. Netherlands Journal of Sea Research, 13: 406–421. https://doi.org/10.4030/jjcs1979.1979.5

Rolet, C., Spilmont, N., Dewarumez, J.M., Luczak, C., 2015. Linking macrobenthic communities structure and zonation patterns on sandy shores: Mapping tool toward management and conservation perspectives in Northern France. Continental Shelf Research, 99: 12–25. https://doi.org/10.1016/j.csr.2015.03.002

838 Savelli, R., Dupuy, C., Barillé, L., Lerouxel, A., Guizien, K., Philippe, A.,
839 Bocher, P., Polsenaere, P., Le Fouest, V., 2018. On biotic and abiotic drivers
840 of the microphytobenthos seasonal cycle in a temperate intertidal mudflat: a
841 modelling study. Biogeosciences, 15: 7243–7271. https://doi.org/10.5194/bg-
842 15-7243-2018

843 Schöttler, U., Wienhausen, G., Westermann, J., 1984. Anaerobic metabolism
844 in the lugworm *Arenicola marina* L.: The transition from aerobic to anaer-
845 obic metabolism. Comparative Biochemistry and Physiology Part B: Bio-
846 chemical and Molecular Biology, 79: 93–103. https://doi.org/10.1016/0305-
847 0491(84)90083-X

848 Schröer, M., Wittmann, A.C., Grüner, N., Steeger, H.U., Bock, C., Paul, R.,
849 Pörtner, H.O., 2009. Oxygen limited thermal tolerance and performance in the
850 lugworm *Arenicola marina*: A latitudinal comparison. Journal of Experimen-
851 tal Marine Biology and Ecology, 372: 22–30. https://doi.org/10.1016/j.jem
852 be.2009.02.001

853 Seuront, L., Ng, T.P.T., 2016. Standing in the sun: infrared thermography
854 reveals distinct thermal regulatory behaviours in two tropical high-shore lit-
855 torinid snails. Journal of Molluscan Studies, 82: 336–340. https://doi.org/10.
856 1093/mollus/eyv058

857 Shumway, S.E., Davenport, J., 1977. Soma espects of the physiology of *Areni-*
858 *cola marina* (Polychaeta) exposed to fluctuating salinities. Journal of the Ma-
859 rine Biological Association of the U.K., 57, 907–924.

860 Smith, K.R., Cadena, V., Endler, J.A., Porter, W.P., Kearney, M.R., Stuart-
861 fox, D., Stuart-fox, D., 2016. Colour change on different body regions provides
862 thermal and signalling advantages in bearded dragon lizards. Proceedings of
863 the Royal Society B: Biological Sciences, 283: 1832.

864 Sommer, A.M., Pörtner, H.O., 2004. Mitochondrial function in seasonal ac-
865 climatization versus latitudinal adaptation to cold in the lugworm *Arenicola*

marina (L.). Physiologial and Biochemical Zoology, 77: 174–186. https://doi.org/10.1086/381468

Thomas, Y., Bacher, C., 2018. Assessing the sensitivity of bivalve populations to global warming using an individual-based modelling approach. Global Change Biology, 24: 4581–4597. https://doi.org/10.1111/gcb.14402

Volkenborn, N., 2005. Ecosystem engineering in intertidal sand by the lugworm *Arenicola marina*. University of Bremen. Ph D Thesis.

Watson, G.J., Murray, J.M., Schaefer, M., Bonner, A., 2017. Bait worms: a valuable and important fishery with implications for fisheries and conservation management. Fish and Fisheries, 18: 374–388. https://doi.org/10.1111/faf.12178

Watson, G.J., Murray, J.M., Schaefer, M., Bonner, A., 2015. Successful local marine conservation requires appropriate educational methods and adequate enforcement. Marine Policy, 52: 59–67. https://doi.org/10.1016/j.marpol.2014.10.016

Watson, G.J., Williams, M.E., Bentley, M.G., 2000. Can synchronous spawning be predicted from environmental parameters? A case study of the lugworm *Arenicola marina*. Marine Biology, 136: 1003–1017. https://doi.org/10.1007/s002270000283

Xenarios, S., Queiroga, H., Lillebø, A., Aleixo, A., 2018. Introducing a regulatory policy framework of bait fishing in European Coastal Lagoons: The case of Ria de Aveiro in Portugal. Fishes, 3: 2. https://doi.org/10.3390/fishes3010002